Aus der Klinik und Poliklinik für Orthopädie

Universitätsklinikum Hamburg-Eppendorf

Direktor Prof. Dr. Wolfgang Rüther

Microcirculatory dysfunctions Present in Early Stages of

Metabolic Alterations in a Diabetic Mouse Model *in vivo*

DISSERTATION

zur Erlangung des Grades eines Doktors der Humanmedizin

dem Fachbereich Medizin der Universität Hamburg vorgelegt

von

Tanja Biermann

aus Singapur

Hamburg, 2005

Angenommen vom Fachbereich Medizin

der Universität Hamburg am: 19.072005

Veröffentlicht mit der Genehmigung des Fachbereichs

Medizin der Universität Hamburg

Prüfungsausschuss, der/die Vorsitzende/r: Prof. Dr. W. Rüther

Prüfungsausschuss 2. Gutachter/in: Prof. Dr. F.U. Beil

Prüfungsausschuss 3. Gutachter/in: PD Dr. S. Ergün

Die vorliegende Arbeit wurde in der Zeit von

November 1999 bis Juni 2005 unter der Leitung von

Dr. Nils Hansen-Algensteadt angefertigt.

meinen Eltern
in Liebe gewidmet

Index

1. Aim of the Study

Microvascular dysfunctions dominate the morbidity and mortality in Type 2 diabetes. However the origin of microvascular dysfunction is a multifaceted process with sequentially occurring functional and morphological alterations. Consequently, it is important to analyze these microvascular alterations with models enabling us to monitor functional and morphological alterations continuously non-invasive in an animal model that mimics the sequential metabolic alterations in diabetic disease.

A previous study showed that functional and morphological microvascular alterations in subcutaneous tissue are present at an early stage of diabetes and that these alterations correlated with the metabolic situation represented by blood glucose levels and bodyweight [1].

The aim of the present study was to analyse the dynamics in the establishment of mirovascular alterations in accordance of the metabolic stages (Syndrome X). Namely whether, microvascular alterations occur before established diabetic metabolic situation or if they lack behind. These insights allowing that in the future, adequate therapeutical intervention can be initiated at the correct time.

A further objective was to identify the acute effect of different causes of microvascular dysfunction, namely hyperinsulinaemia, hyperglycaemia and dyslipidaemia.

2. Background

2.1 Obesity, Metabolic Syndrome and Diabetes Mellitus

Obesity, leading to insulin resistance, metabolic syndrome and consecutively diabetes mellitus Type 2, with its complications, has become a serious problem over the last decades.

The leading cause of morbidity and mortality in patients with diabetes mellitus are accelerated vascular complications in both micro- and macrovasculature [2]. Microvascular complications are often present when diabetes is diagnosed, with high prevalences of 20% retinopathy, 9% neuropathy and 1% diabetic nephropathy [3]. The basic underlying abnormalities are due to abnormal vascular function of both micro- and macro vascular tissues, involving mainly for microvessels, the classic tissues retina, renal glomeruli [4], peripheral nerves vasculature, skin and cardiovascular system. Frequently, vascular complications are already manifested when diabetes is uncovered, even in patients without symptoms. Diabetes is defined as blood glucose values >110mg/dl after fasting and values >200mg/dl during a two hours oral Glucose Tolerance Test (OGTT), according to German Diabetes Association (Deutsche Diabetes-Gesellschaft) and metabolical syndrome (MS) is defined as a clustering of risk factors (triglycerides, glucose, high-density lipoprotein cholesterol, blood pressure (BP), abdominal obesity) by the National Cholesterol Education Program (NCEP). Not only is there a correlation between diabetes associated mortality, blood glucose and OGTT values

[5], but it also has been shown that the incidence of vascular complications rise with the duration of the disease [6].

Different risk factors to develop vascular dysfunctions have been identified, among them hyperglycaemia, hyperinsulinaemia, hypercholesterolaemia and elevated triglyceride levels, described in more details in the following subchapters.

Given the diversity of involved risk factors, it is unlikely that any single causal factor explains the known vascular changes present in diabetic complications.

2.2 Vascular Dysfunction, Angiogenesis and functional and morphological Microvascular Parameters

The formation of new blood vessels (angiogenesis) plays an important role during development, physiological repair processes, and various diseases such as diabetic retinopathy and growth of solid tumors [7, 8]. Angiogenesis is regulated by a balance of positives and negative factors of blood vessel growth. Positive factors include acidic Fibroblast Growth Factor (aFGF), basic Fibroblast Growth Factor (bFGF), Vascular Endothelial Growth Factor (VEGF), angiotensin and others [9]. Formation of collateral blood vessels in ischaemic limbs or in ischaemic myocardium may depend for instance upon hypoxic upregulation of VEGF production

[10]. Furthermore it has been postulated that VEGF may be a major mediator of ocular neovascularization in diabetes [11].

Tumor Necrosis Factor-alpha (TNF-α) is known to increase dose-dependent the expression of adhesion molecules such as E-Selectin, Vascular Cell Adhesion Molecule-1 (VCAM-1) and Intercellular Adhesion Molecule-1 (ICAM-1) in dermal endothelial cells [12] as well as in intestinal microvascular endothelial cells [13]. It has been observed that local application of TNF-α increases Leukocyte-Endothelial-Interaction (LEI) without altering heamodynamic parameters in subcutaneous tissue [14]. Wound healing processes have been shown to be slower and angiogenesis reduced when TNF-α levels are increased in high non physiological levels [15]. Furthermore elevated TNF-α plasma levels have been found in obese humans [16].

It has been shown that functional alterations precede and determine morphological changes of the microcirculation [17]. Microvascular dysfunction is a sequential alteration where functional abnormalities, such as increased permeability, entrapment of leukocytes and alteration in blood flow rate, are first present and morphological changes, such as lower vessel density and increased vessel diameter, develop later [18, 19]. Previous studies in diabetic patients show endothelial dysfunction and functional alterations in the microcirculation. Animal models were characterized by increased vascular permeability [20], alteration in erythrocyte velocity [18], sequestration of leukocytes [18, 21, 22] and morphological alterations such as altered vascular density [18].

Permeability of vessels for albumin is one of the most sensitive parameters being the primarily affected microvascular dysfunction [23, 24]. Altered permeability governs substrate delivery via changes in transendothelial transport and increased interstitial pressure leading to an edema [25]. In the eye, for instance neovasculsarisation in combination with the increase of vascular permeability, leads to the damages in the retina and nervus opticus [18, 26]. Furthermore changes in vascular permeability lead to an altered viscosity of the blood and influences Leukocyte-Endothelial-Interaction (LEI).

A previous study [1] has shown that an increased permeability in the microvasculature of subcutaneous tissue, in uncoupling protein promoter-driven diphteria toxin A transgenic (UCP1/DTA) mice, can already be observed in the early-stage of the diabetic disease. Multiple other studies have seen that, in retina [27], kidney [28] and rat mesentery [5, 18, 29, 30], increased permeability to albumin is an early endothelial dysfunction in diabetes.

Leukocytes entering a blood vessel may continue to float with the blood flow, roll along the vessel wall, adhere transitorily or permanently with the vessel wall or extravasate out of the vessel. Local hydrodynamic and adhering forces regulate these interactions. The hydrodynamic forces are determined by vessel diameter, blood flow velocity, and viscosity. Adhering forces are regulated by the quantity, strength and kinetic of links between adhesion molecules on the leukocyte and the endothelial surface. Cell deformability influences both forces [14, 31, 32]. There are

two major families of Cell Adhesion Molecules (CAMs) which play a role in leukocyte rolling and adhesion. Selectines (p, l and e) mediate the rolling while immunglobulin G (IgG) family members (ICAM-1 and VCAM-1) expressed on endothelium cells with cognate receptors (beta2 and beta1 intregrin Receptors) on leukocytes mediate the stabile adhesion. The CAM expression on endothelium cells and leukocytes can be modulated by cytokines expressed from different cells (tumour cells, fibroblasts, macrophages).

An increased LEI is known to increase ischemia-reperfusion damage, capillary nonpefusion, and to trigger neovascularisation in the eye among others [18, 36, 37]. In diabetic rats an increased leukocyte entrapment in the living retina, in the early stages of diabetes, was shown to lead to microvascular occlusion and dysfunction [22].

Following the functional alterations we have the morphological changes such as vessel density, diameter and branching pattern of the vessels. Decreased vessel density results in a reduced area for possible substrate transport. An increased vessel diameter, when not accompanied with proportional alterations of vessel density and blood flow rate, can lead to a slower perfusion rate, which equally interferes with an adequate substrate delivery. The prior study performed with UCP1/DTA mice with early-stage diabetes showed decreased vessel densities and higher diameters resulting from a shift towards larger diameters, indicating a decreased number of small vessels. These alterations lead to altered hydrodynamic forces, such as share rate. Interestingly it was shown that the decreased

shear rate could only be partially responsible for the shown increased LEI, which continued to rise with higher blood glucose levels, even when shear rates reached a plateau. The other microvascular parameters in the study equally showed a close correlation between microvascular alterations and blood glucose values [1].

Changes in morphological parameters can induce through its influence on the perfusion of an area, metabolical alterations such as pathological pH levels and hypoxia among others. Hypoxic microenvironment is a stimulus for angiogensis, up-regulating expression of factors such as VEGF among others linked to angiogenesis [38-42].

The altered microenvironment, which is a consequence of this intertwined cluster of parameters, namely vessel diameter, vessel density, blood flow rate, microvascular permeability and LEI, and its alterations, produces an impaired reaction to substrate demand in tissue, especially under stress situations such as wound healing [43], inflammation or even physiological states such as growth [44].

2.3 Hyperglycaemia, Hyperinsulinaemia, Dyslipidaemia and their Role in Vascular Dysfunction

2.3.1 Hyperglycaemia

Amongst the risk factors for vascular disease, abnormalities in insulin and glucose metabolism and dyslipidaemia, play an important role in the dynamic of pathology in vascular cells [45]. Hyperglycemia has been shown to be a cause of microvascular complications in diabetes [46, 47]. The mechanisms by which high glucose concentrations may induce vascular changes in diabetic patients are not well understood, however it has been described previously in clinical trials such as the Diabetes Control and Complication Trial (DCCT) and the Epidemiology of Diabetes Interventions and Complications (EDIC) [47-49] that intensive therapy, with the aim of maintaining blood glucose and glycoslated hemoglobin concentrations as close to normal range as possible, reduces the risk of progressive retinopathy and nephropathy [50].

Multiple mechanisms have been suggested for the possible pathway by which hyperglycemia could cause vascular dysfunction such as advanced glycation end products [51], sorbitol-myo-inositol changes [52], increased synthesis of diacylglcerol (DAG) [53] and alterations in DAG-Protein Kinase C (PKC) pathway activation [54]. PKC is associated with abnormal vascular cell functions in diabetes, including cell contraction, capillary basement membrane thickening, which is characteristic for diabetic

microangiopathy [55], altered signal transduction of hormones, growth factors [56, 57], and cell proliferation [58-65].

It has been observed that persistent hyperglycemia can accelerate the formation of advanced glycation end-products, known as a trigger to arterial inflammation [51]. Furthermore several mechanisms including direct effects on cellular signaling pathways and diminished Na+, K sup+-ATPase activity, have been suggested [52]. It has been observed that glucose induced PKC activation interferes with agonist-induced intracellular calcium signaling [61]. The family of PKC include at least 11 isoforms [66]. Among the various PKC isoforms the ß and γ isoforms appear to be activated preferentially in the vasculatur of diabetic animals, for instance in aorta and heart of diabetic rats [53] and in cultured aortic smoth muscel cells exposed to high levels of glucose [67], although other isoforms are also increased in the renal glomeruli and retina [68, 69].

The detection of increased concentrations of several growth factors (GF) in the target tissues of diabetic long-term complications, supports the speculation that a number of aberrantly expressed GF have a role in the development of these complications [70]. The enhanced expression of GF, consequently activate the biological pathways, linking hyperglycaemia to microvascular changes (polyol pathway; non-enzymatic glycation of proteins; vasoactiv hormones; oxidative stress and hyperglycaemic pseudohpoxia).

Other reports have shown that the expression and the actions of growth factors such as Vascular Endothelial Growth Factor (VEGF) and Epidermal Growth Factor (EGF) can also possibly be regulated by PKC activation in vascular cells.

It has been observed that endothelial dysfunction is associated with hyperglycaemia in diabetes mellitus patients with and without microalbuminuria, suggesting that the endothelial dysfunction may precede the clinical manifestation of diabetic microangiopathies [71]. Concerning functional microvascular parameters it has been shown that *in vitro* high glucose concentrations can activate PKC in endothelial cells, resulting in a stimulated expression of adhesion molecules facilitating the adhesion and uptake of leukocytes, and that high concentrations of glucose affect permeability of tight junctions. These results emphasizes the importance of postprandial glucose spikes in the early development of micro- and macrovascular disease [72].

2.3.2 Hyperinsulinaemia

The role of the endothelium in insulin action has been increasingly recognized [73]. There are different hypothesis mechanisms but none fully explain the clinical situation. This might be due to a lack of appropriate models, a complete analyzes of the multifaceted, time course dependent process represents an inexorable problem.

Insulin is supposed to have a direct vasodilatory role at the level of the skeletal muscle arteriole [46], by this path increasing hormone and substrate supply to the interstitial space. Functionally, infusion of insulin has been shown to cause dose-dependent vasodilatation (half maximal response ~40µU/ml), possibly via the stimulation of nitric oxide [74]. It is clear from both in vivo and in vitro studies that insulin may have multiple actions on the vasculature in physiological conditions. However, very little is known regarding the insulin signal transduction mechanism in the vasculature and whether insulin resistance actually exists in the vasculature itself.

Most of the postulates on the mechanisms by which insulin causes vascular dysfunction are based on the assumption that insulin resistance induces hyperinsulinaemia. The elevated level of insulin in turn causes abnormalities of the vasculature. This postulate is only feasible if there is a different mechanism of resistance *in vivo*, with vascular tissue lacking the resistance to insulin. Otherwise hyperinsulinaemia should not have any more effect on the vasculature than it does on the classical insulin tissues. Alternatively, it is possible that it is the lack of insulin effect on vasculature that causes the vascular dysfunction and not the hyperinnsulinaemia. This would predict that insulin regulates a wide spectrum of actions on the vasculature, including metabolic effects. In addition, insulin can mediate chronic effects, such as mitogenic actions through both insulin and insulin like growth factor 1 [75]. In the insulin resistance state, the lack or diminished level of insulin actions will mostly influence its metabolic

effects, as exemplified by the stimulation of glucose metabolism and possibly nitric oxide production for vasodilatation. The lack of insulin's metabolic actions will allow other vasoconstrictors to mediate their effect unopposed. Together with the hyperinsulinaemia, which could enhance the mitogenic effect of other growth factors via insulin-like Growth Factor 1 (IGF-1) receptor, the presence of resistance to insulin's metabolic actions on the vascular tissue leads to vascular dysfunction.

2.3.3 Dyslipidaemia

Apart from insulin and glucose the effect of dyslipidaemia on vessels and endothelial dysfunction has been discussed intensively [76].

The lipid triad (elevated triglycerides, decreased High-Density-Lipoprotein (HDL) cholesterol and increased small dense Low-Density-Lipoprotein (LDL) cholesterol) is a powerful risk factor for artherosclerosis in Type 2 diabetes [77]. The prevalence of hypertriglyceridaemia is three times higher in Type 2 diabetes. It promotes vascular risk directly as well as indirectly through association with alterations of lipoprotein size and composition [78].

It has been shown in the Risk Factors in Impaired Glucose Tolerance for Atherosclerosis and Diabetes (RIAD) study [79], that plasma triglycerides significantly increased and HDL-cholesterol decreased in the 4th and 5th quintiles of a two hour oral glucose tolerance test in subjects at risk for the development of Type 2 diabetes. Furthermore patients with diabetes are

more likely to suffer postprandial hyperlipidaemia [76]. The relationship between hypertriglyceridaemia and diabetes mellitus Type 2 could be explained, according to the lipocentric view of the etiology of Type 2 diabetes, with primary defects in triglycerides and fatty acid metabolism leading to insulin resistance and the lipotoxid effect of free fatty acids, possibly responsible for cell destruction.

Triglycerides have proven to be an independent risk factor in some studies [77, 80, 81]. Furthermore it has been shown that impaired insulin action leads to increased rates of intracellular hydrolysis of triglycerides with the release of nonesterified fatty acids (NEFA). NEFA provides substrate for the liver, in the presence of impaired insulin action and relative insulin deficiency, a base for the complex alterations in plasma lipids [82]. Plasma VLDL levels are raised, LDL-c particles become small and dense, held to be more athrogenic than larger counterparts because they are more liable to oxidation and may more readily adhere and subsequentially invade the arterial [82, 83].

This has been supported by *Fabryova et al.* who showed that if serum triglycerides exceed a certain limit, there is an increase in small, dense LDL [84].

Supporting these hypothesis trials, of lipid-lowering therapies showed that diabetic subgroups benefit more than those without diabetes [83, 85]

An early response induced by hypercholesterolemia is an increase of vascular cell adhesion molecule-1 (VCAM-1) [86]. It has been seen that

oxidized Low-Density-Lipoprotein (oxLDL) and its oxidized lipid components are cytotoxic for endothelial cells [87] as well as inhibiting nitric oxid and increasing expression of VCAM-1 [88]. Modified lipoprotein particles can induce transcriptional activation of VCAM-1. Pro-inflammatory cytokines, such as interleukin (IL)-1 beta or Tumor Necrosis Factor-alpha (TNF-α), induce VCAM-1 expression in endothelial cells [89]. In the metabolic syndrome, Low-Density-Lipoprotein (LDL) levels often remain in the average range, although the particles may have qualitative alterations that render them small and dense, making them particularly vulnerable to oxidation and hence evoking inflammation. Low levels of High-Density-Lipoprotein (HDL) that characteristically accompany the elevated triglycerides in the metabolic syndrome diminish another endogenous anti-inflammatory and hence atheroprotective mechanism [90].

2.4 Intravital Microscopy

Prerequisites for an *in vivo* observation of morphological and functional microvascular parameters are: Tissue preparation, allowing a cell observation, non-toxic optical labels, which are specific for the cell population, technical materials for the measurement for leukocyte flux, rollers, stickers, as well as cell flow in the observed vessel.

To measure gene expression, functional and morphological parameters there are traditionally two choices: the use of an invasive technique, requiring tissue excision, or non invasive techniques, which have low spatial resolution (e.g. MRT; range: mm-cm). The former limits the ability to obtain temporal dynamics, the later excludes visualization at the cellular and subcellular level (1-10μm). Furthermore a combined evaluation of functional and morphological aspects is an evident problem of low magnification non invasive techniques such as MRT (range: mm-cm). Intravital microscopy can overcome these limitations. It provides insight in molecular and cellular processes *in vivo* with high spatial and unlimited temporal resolution.

Our and other groups established methods for repeated, non-invasive observation and quantification of angiogensis in mice. For measurement of vessel diameter and red blood cell (RBC) velocity, fluoroscein isothiocyanate labeled dextran was used as a plasma tracer. Endogeneous leukocytes were visualized in vivo by intravenous injections of the fluorescent marker rhodamin-6-G. Measurements of effective

microvascular permeability to albumin were performed by fluorescence microscopy in aid of a photomultiplier [91].

By intravital microscopy, the density of functional vessels in tissue can be most accurately quantified by measurement of functional vascular density and the total length of perfused microvessels per unit area of observation. Furthermore intravital microscopy visualizes geometric and hemodynamic characteristics of newly grown vessels as well as leukocytes interacting with the endothelium [14].

Intravital microscopy permits acute observations, which consist of one time measurements, as well as chronic measurements allowing an observation of a field over a period from days to months.

The mostly used acute preparation is messenterica or creamaster muscle of rodents [92]. These techniques do not allow a continuous assessment of microvascular properties contrary to the chronicle preparations, suzch as that of rabbit ear [93-96], dorsal skinfoldchamber [97, 98] in rodents, cranial windows in mice or rats [14, 99, 100] and femur window in mice [101].

2.5 Diabetic Mouse Model

Transgenic uncoupling protein promoter-driven diphtheria toxin A (UCP1/DTA) mice, characterized by severe brown adipose tissue (BAT) deficiency with consecutively reduction of energy expenditure, were used for this study [102, 103]. As animals age, they develop marked obesity, insulin resistance, hyperglycaemia, hyperlipidaemia, leptin resistance, and hypertension, thus resembling the complete metabolic syndrome of obese humans [104, 105].

Brown adipose tissue (BAT) has been proposed to play an important role in the regulation of energy balance of rodents. BAT is distinguished by the unique presence of an uncoupeling protein (UCP), a mitochondrial proton transporter that uncouples oxidative metabolism from ATP synthesis. This permits BAT to expend calories unrelated to the performance of work with the result being the generation of heat. BAT activity is stimulated during cold exposure (nonshivering thermogenesis) and during ingestion of excess calories (diet-induced thermogenesis) [106-110].

The genetic toxigene ablation technique was used to create mice with isolated brown fat deficiency [102]. This was accomplished by using a suicide DNA transgenic vector in which regulatory elements of the UCP gene were used to drive BAT specific expression of diphtheria toxin A-chain (DTA). It has been shown that raising at thermoneutrality prevents the development of obesity [111, 112], and that UCP1/DTA mice are less cold resistant [102, 113].

At the age of 16 days transgenic UCP1/DTA mice have pronounced reduced functional brown fat mass, characterized by a 68% decrease in UCP content of the interscapular brown fat depot compared with that of none transgenic littermates. This is accompanied by moderate obesity, with a 31% increase of total body lipid. Initially the obesity develops in absence of hyperphagia, demonstrating that the mice have decreased energy expenditure.

At the age of eight weeks transgenic mice develop hyperphagia in addition to decreased thermogenesis causing obesity, severe insulin resistance, as evidenced by hyperinsulinaemia and hyperglycaemia, hypertriglceridaemia and hypercholesterolaemia. These manifestations occur sequentially and at the age of 12 weeks UCP1/DTA mice are obese, and are, in absence of elevated blood glucose levels, characterized by insulin resistance, hyperinsulinaemia and dislipidaemia, parameters of the metabolic syndrome.

In a previous study [1] 20 week old mice were used to mimic the early-stage diabetes, since mice at the age of 22 weeks have an average increase of 54%/75% (male/female) in body weight, 30% in blood glucose levels, and 85- to 125- fold increase in blood insulin levels.

For this study 12-week-old UCP1/DTA mice were used to mimic the initial state of diabetes, where impaired glucose tolerance is one of the few signs present, known to demonstrate an increase in food intake of

29%/27% (male/female), and possessing a 69-75% reduction of BAT and 10.1g/9.5g (male/female) bodyweight increase.

It is known that male and female did not display significantly higher glucocorticoid levels than control mice of the same age. Previous studies showed significantly increased triglyceride levels in 20 week old mice on chow diet with a stronger increase when feed western diet. However, cholesterol levels only showed a significant increase when mice were feed western diet, and non-significant differences compared to controls when feed chow [113].

Plasma insulin levels in male at the age of 12 weeks were noted with 74.9 $\pm$ 19.6 ng/ml versus 1.53 $\pm$ 0.40 ng/ml, 49-fold in controls, while female mice at 12 weeks had smaller differences with insulin levels of 2.92$\pm$1.23 ng/ml versus their control littermates with 0.54$\pm$0.15 ng/ml.

The obese UCP1/DTA mice have many features in common with obesity as it appears in most humans without displaying features found in other mouse models that are not present in humans suffering from Diabetes such as reduced fertility or infertility, stunted linear growth, decreased lean body mass, and elevated glucocorticoides. This makes them an ideal animal model for studies of obesity- associated insulin resistance and non-insulin dependent diabetes mellitus and the related complications.

3. Material and Methods

3.1 Study design and Technical Setup

3.1.1 Study design

Dorsal skin-fold chambers were implanted in 12 week old, UCP1/DTA mice and control litter mates. Mice were held under controlled temperature (24°C) and humidity (50%) and with water and standard rodent chow (chow number S5714S040; Sniff, Soest, Germany) available *ad libitum*. All animal procedures were performed according to the German animal welfare committee (Tierversuchsantrag Genehmigungsnummer 15/2000, Gesundheitsamt und Soziales Amt für Gesundheits- und Veterinärwesen Hamburg, Germany). During the experiments and surgical procedures, mice were anesthetized with ketamine and xylaine (7.5 mg ketamine hydrochloride, Ketanest®, Parke-Davis, Berlin/Germany and 2.5 mg xylazine hydrochloride, Rompun 2 %®, Bayer Vital, Leverkusen/Germany, per 100 mg bodyweight).

Prior to chamber implantation a glucose-tolerance-test (G-G-T) was performed (Figure 1). Measurements of bodyweight, temperature, blood glucose levels and assessment and digital documentation of the chamber were performed on the day of surgery as well as on the 3, 6 and 9 after chamber implantation. Epifluorescent techniques were employed to monitor effective microvascular permeability, vessel density, vessel

diameter, blood flow rate, and leukocyte-endothelial-interaction repeatedly on days 6 and 9 after surgery.
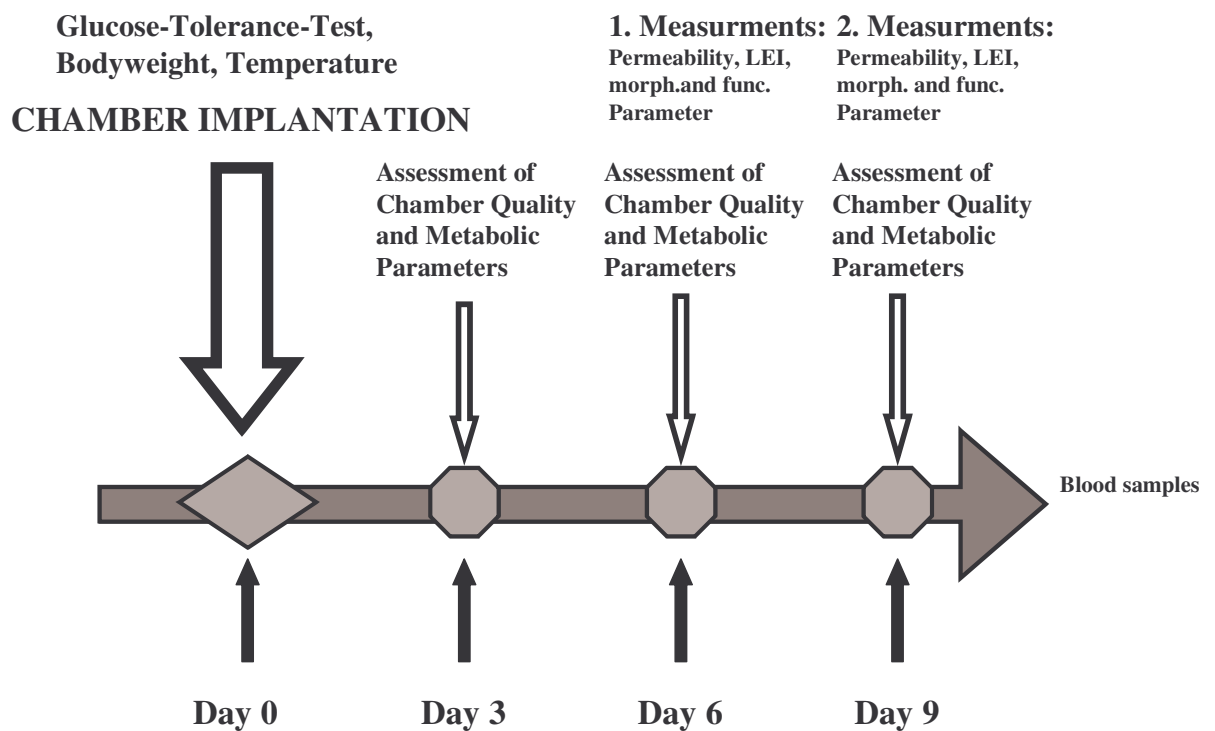
STUDY DESIGN

Glucose-Tolerance-Test, Bodyweight, Temperature

CHAMBER IMPLANTATION

1. Measurments: Permeability, LEI, morph.and func. Parameter

2. Measurments: Permeability, LEI, morph. and func. Parameter

Assessment of Chamber Quality and Metabolic Parameters

Assessment of Chamber Quality and Metabolic Parameters

Assessment of Chamber Quality and Metabolic Parameters

Blood samples

Day 0   **Day 3**   **Day 6**   **Day 9**

Figure 1. Study Design

Intravital microscopy was performed on day 6 and 9 after chamber implantation along with the assessment of chamber quality and metabolic values which were performed furthermore on day 0 and 3.

3.1.2 Tracer Molecules and Optical System

Intravital measurements were performed using a fluorescence microscope (Axioplan; Zeis, Oberkochen/Germany) and 1.25x, 2.5x, 10x and a 20x long working distance objectives (Zeis, Oberkochen/Germany). The microscope is equipped with fluorescence filter sets for fluorescein isothiocyanate dextran (FITC-Dextran, MW 2 million, peak excitation: 488nm, peak emission: 515-545nm, Sigma-Aldrich) and rhodamine (Rho-6-G, MW 479.02 and Rho-BSA, tetramethylrhodamin conjugated Bovine Serum Albumin, MW 67000, peak excitation: 544nm, peak emission: 572nm, Molecular Probes, Leiden/Netherlands).

Microcirculatory parameters were monitored using a charge couple device (CCD) camera (C2400-97), a camera-controller (C2400, Hamamatsu Photonics, Hersching/Germany) a, and a computer (Apple Power MacIntosh, G4, Dual 500 MHz) for non-compressed digital signal recording and off-line analysis. Furthermore a photomultiplertube (R4632 Hamamatsu Photonics, Hersching/Germany) for light intensity messurements connected to an analog-digital converter (Powerlab/200, Chromaphor Analysen Technik GMBH, Duisburg/Germany) was also coupled with the computer system enabling off-line analysis of the acquired data (Figure 2). For documentation of chamber quality on various days during the study a digital camera (AxioCam, Zeiss, Göttingen/Germany) was connected to the microscope.
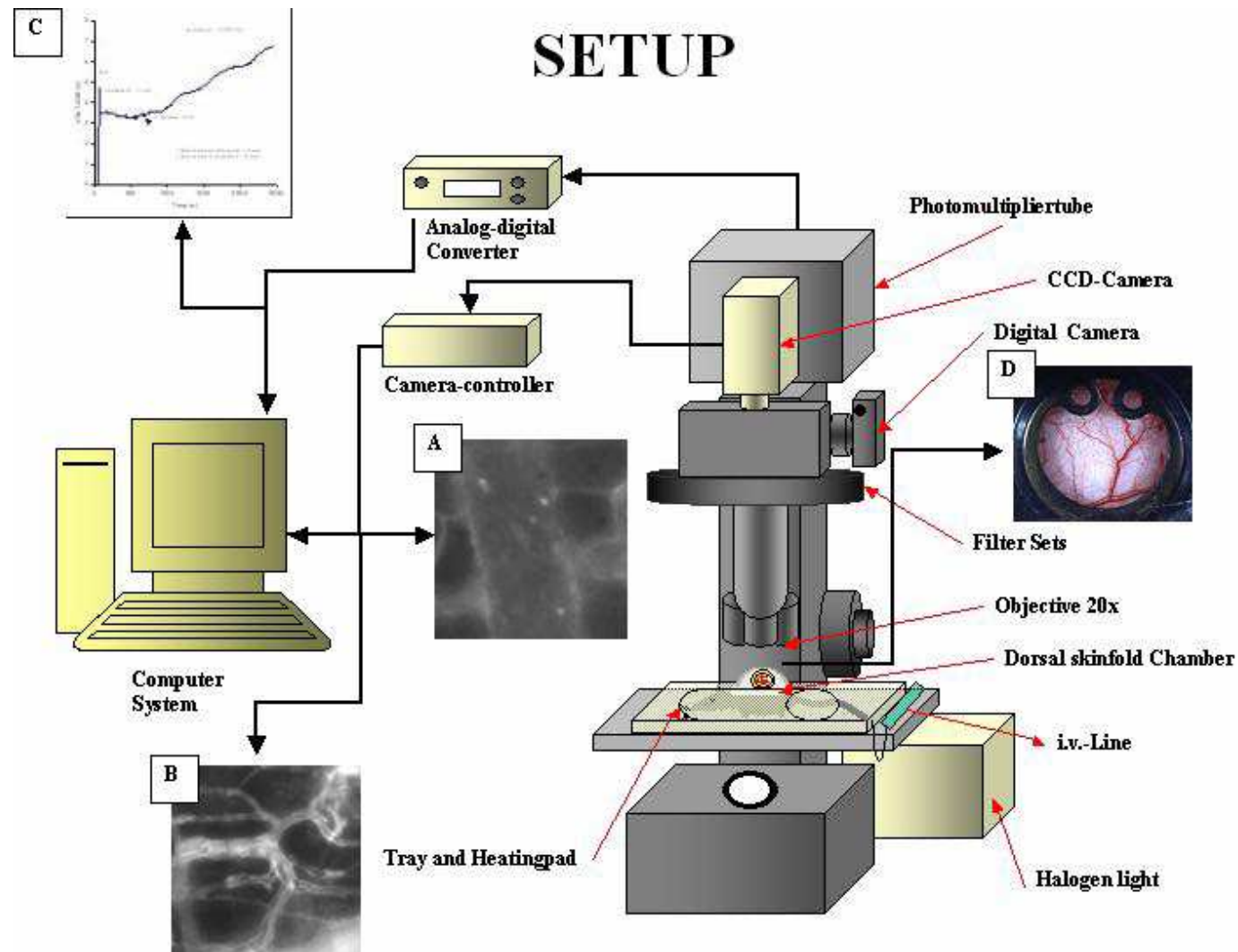
Figure 2. Experiment setup consisting of a optical system and computer enabling off–line analyze with an image processing system. With help of fluorescein filter-sets, microscope images of leukocytes (A) and plasma flow (B) in functional vessels are captured with the CCD-Camera and digitally recorded. Permeability (C) was assessed with help of a photomultiplertube, measuring fluorescein intensity, and a analog-digital converter offering data for calculation, resulting visually in a curve. A digital camera for chamber overview pictures (D) was connected to the microscope.

3.2. Metabolic Parameters and Serum Levels

3.2.1. Bodyweight, Blood Glucose, Temperature and Glucose-Tolerance-Test (GTT):

Bodyweight (scale model 936 B-2, Korona GMBH, Moringen/Germany), rectal body temperature (Thermalert TH-5, Phyitemp, Clifton/USA) and whole blood glucose levels were measured on the day of chamber implantation and on days 6 and 9 after chamber implantation. Prior to chamber implantation glucose-tolerance-tests (GTT) were performed to verify the existing pathological glucose tolerance in UCP1/DTA mice versus controls. Therefore food was withdrawn for 8 hours, a baseline blood sample was collected via puncture of one of the tail veins with a heperanized capillary and glucose (1mg/g bodyweight, 100mg glucose/1ml PBS: 0.6 M) was administered by intraperitoneal injection. Additional whole blood samples were obtained at indicated time points (15min, 30min, 60min, 90min and 120min) after glucose administration, resulting in 6 values for the assessment of glucose tolerance. Blood glucose was determined using glucose oxidase method (Lifescan, ONE TOUCH II, Ortho Diagnostic Systems, Neckargemünd/Germany).

3.2.2 Total Triglyceride, Cholesterol, free fatty acids and fast performance liquid chromatography (FPLC)

Measurements of lipids, FPLC and isolation of cholesterol and triglycerides were done in collaboration with A. Niemeier (Zentrum für Experimentelle Medizin, Institute für Biochemie und Molekularbiologie II, Director Prof. Dr. physiol. Dr. h.c. U. Beisiegel).

Blood was taken by puncture of the retroorbital plexus of five 12 week old male UCP1/DTA mice after 8 hours nighttime fasting. Blood samples where then centrifuged at 3000 turns/minute and 4°C for 15 minutes Serum was then collected. Plasma triglycerides (TG), cholesterol and free fatty acids were determined using commercial enyzme-based kits adapted to microtiter plates (Wako Chemicals, Neuss/Germany (fatty acids); Roche, Mannheim/Germany (TG and cholesterol)). For total triglyceride and cholestrol the experiment was repeated on two separate occasions with different animals (n=10).

To analyze the lipoprotein profile, 200µl pooled plasma samples were separated by fast performance liquid chromatography (FPLC) gel filtration on a Superose 6 column (Amersham-Bioscience), followed by a determination of cholesterol and triglycerides in each fraction. The experiment was repeated on two separate occasions with different animals.

3.2.3 Isolation of TRL (triglyceride-rich lipoprotein) and HDL (high-density lipoprotein)

For injections, serum of UCP1/DTA mice was collected using the same methods as described above. Lipoproteins were isolated by sequential ultracentrifugation with potassium bromide density solution [114, 115], desalted with PD 10 column (Amersham Bioscience) and TG and cholesterol was determined within the single lipoprotein fractions.

To gain the necessary amount of lipoproteins so that systemic application could be performed in the desired concentration, a large number of animals was necessary (n=20).

3.3 Microvascular Parameters

3.3.1 Dorsal Skin-fold Chamber Preparation

Dorsal skin-fold chambers were implanted enabling non-invasive measurements of microvascular parameters *in vivo* [25, 42, 91, 116]. For the surgical procedure animals were anaesthetized as described on page 20. Mice were then shaved (BaByliss, Paris/France) and depilated (Sally Hansen, Del Laboratories/USA) to prepare the skin for dorsal skin-fold chambers implantation (3.2g, Machine shop, Massachusetts General Hospital Boston, USA). Procedures were performed at aseptic conditions and body temperature maintained at physiological levels using a heating pad (Omnilab PST 100, Jürgens).

First one of the titanium frames was temporarily sutured (Ethibond Excel 5/0, Johnson & Johnson, Brussels/Belgian) on the dorsal skin of mice. Skin was gently extended so that a double-layer was produced, followed by the preparation of channels for the two lower positioned screws. Once this was accomplished a circular area of skin was removed so that the microsurgical preparation could be performed using a microscope (Stemi 1000, Zeiss, Oberkochen/Germany) to remove superficial layers allowing a direct view of subcutaneous vessels. The next step consisted in mounting the second frame, fixating it with suture and 3 screws, removing the temporary sutures and placing a glas-coverslip fastened with a ring so that the chamber was airtight. The chamber at this point allows a clear view of subcutaneous tissue and striated muscle of the not prepared

opposite laying skin layer (Figure 3). To avoid a postoperative drop of body temperature mice were maintained on the heating pad until they were completely awake and mobile. Mice showed no signs of discomfort or pain.

Mice were allowed to recover from the chamber implantation for a period of 6 days and only chambers meeting the criteria of intact microcirculation [42] without any optical signs of inflammation, such as redness, pus, edema, swelling or necrosis, were measured.
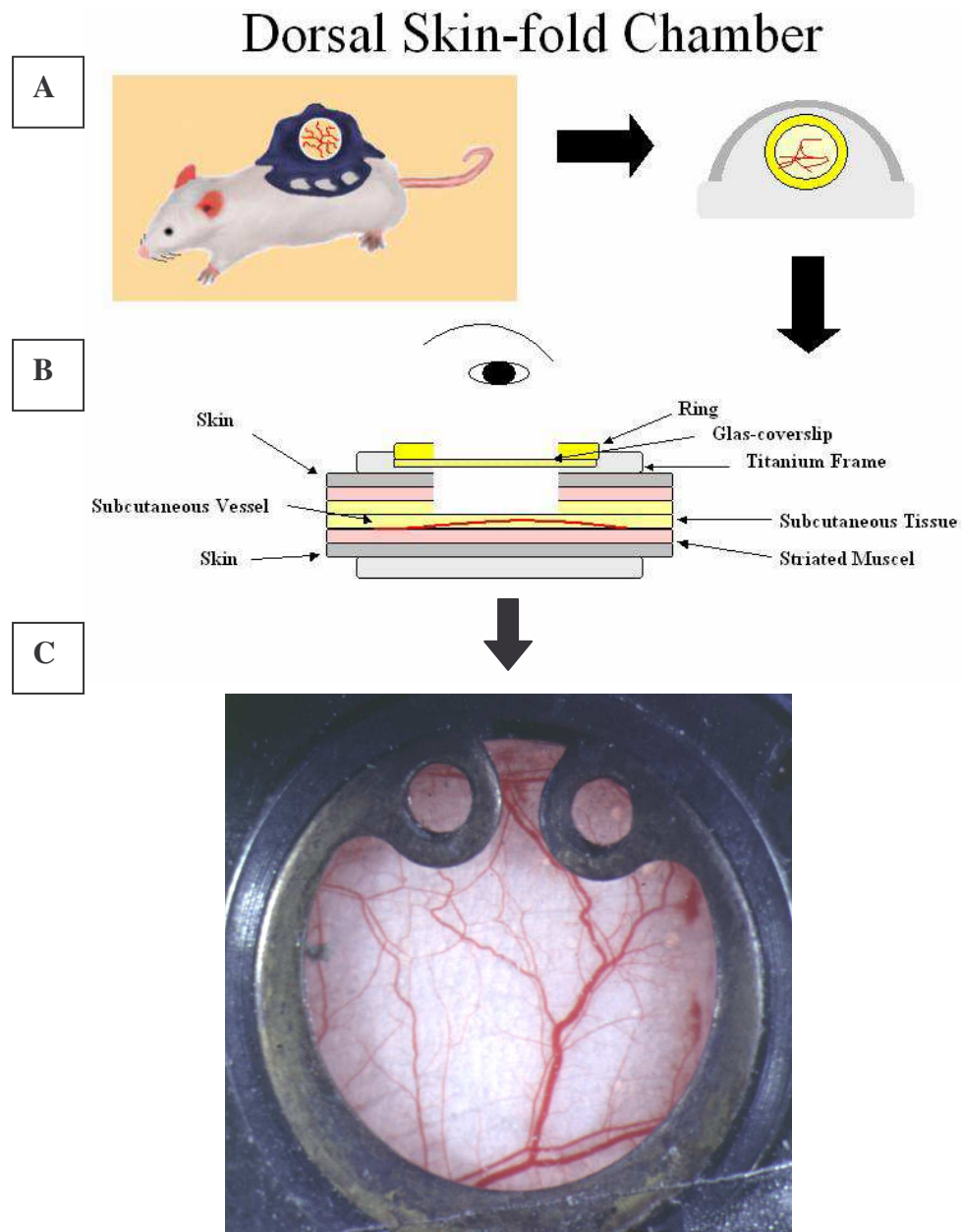
Figure 3. Dorsal skin-fold chamber enabling a view of microvessels of the subcutaneous layer. **A.** Schematic drawing of a mouse bearing a dorsal skin-fold chamber. **B.** Schematic drawing showing the different layers. **C.** Representative picture of an implanted dorsal skin-fold chamber.

3.3.2 Preparation for measurements of microvascular parameters

To allow an intravenous administration of fluorescein and other substances over the period of the measurements, it was necessary to place an i.v. line in one of the 4 tail veins of the mice prior to measurements. For this purpose mice were shortly anesthestized intraperitoneal as described on page 20. Using a polyethylene tube and 30-gage needles we constructed an i.v. line that could be applied to the mouse tail and fixated temporarily for the necessary time to perform the intravital measurements.

3.3.3 Functional Vascular Density (VD), Vascular Diameter (D), Red Blood Cell Velocity (VRBC) and Blood Flow Rate (BFR):

For vessel visualization, a 100 µl bolus of fluoresceinisothiocyanid marked dextran (FITC-Dextran, 50 mg/ml 0,9% NaCl, molar mass 2.000.000, Mobitec / Taufkirchen, Germany), was administered intravenously through the tail vein, marking plasma and by this way clearly visualizing vessels with flow. FITC-fluorescence images were recorded for 30 seconds and analyzed off-line (Figure 4).
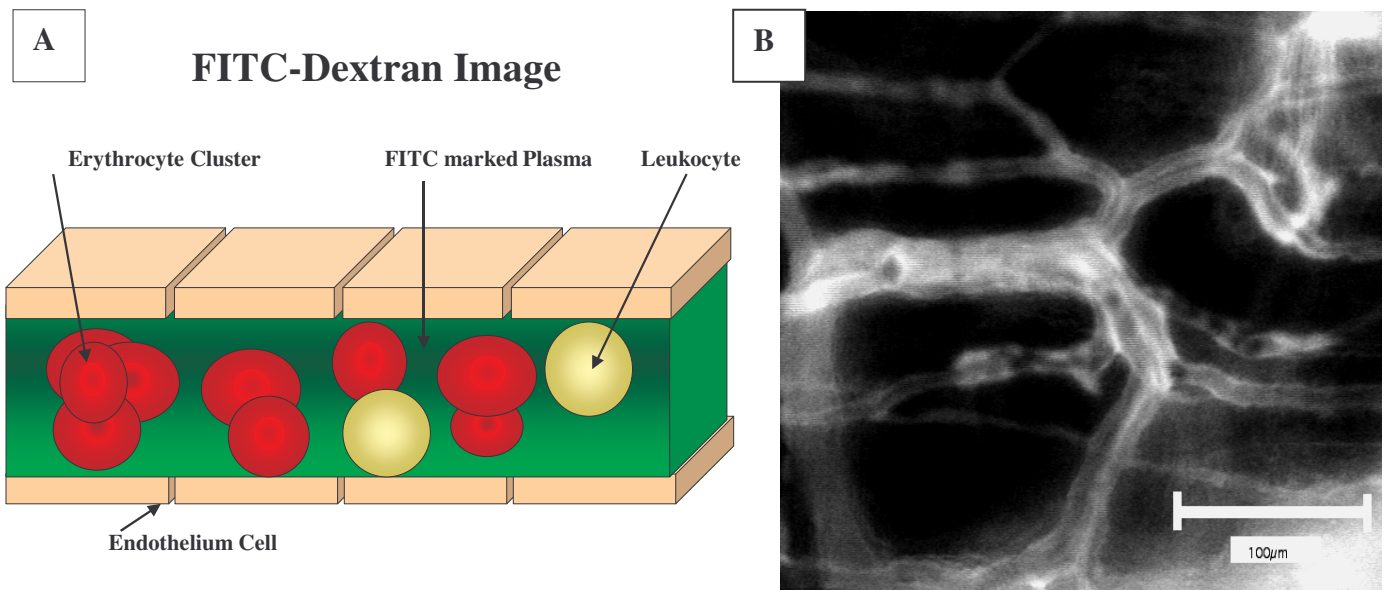
Figure 4.A. Schematic drawing demonstrating how marked plasma is used to visualize vessel for determination of Functional Vascular Density (VD), Vascular Diameter (D), Red Blood Cell Velocity (VRBC), Blood Flow Rate (BFR) using FITC-Dextran. **4.B**. Cells in the blood flow can be clearly identified through the contrast to plasma staining. 20x (Zeiss, Oberkochen/Germany).

Measurements were repeated 4 times in defined areas until data was acquired for 5 fields spread about the chamber so that a mean could be calculated (Figure 5).
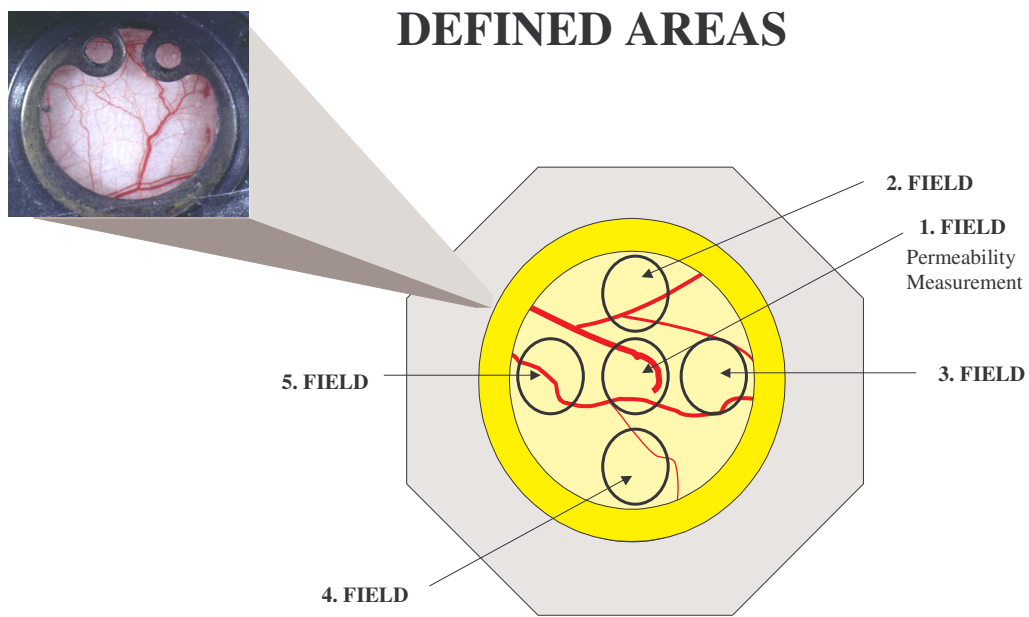
DEFINED AREAS

Figure 5. Dorsal skin-fold chamber. Five fields in areas central and in each corner are used so that a mean could be established.

Functional vessel density (VD) was defined as the sum of length of vessels with a plasma flow per observation area (cm/cm^2).

$$VD\ (cm/cm^2) = \frac{1}{G}\sum_{X=1}^{G}\left[\frac{1}{A}\sum_{n=1}^{Z}L_n\right]_x$$

Mean functional vessel diameter (D) was calculated with the following equation:

$$D\ (\mu m) = \frac{1}{G}\sum_{x=1}^{G}\left[\frac{1}{Z}\sum_{n=1}^{Z}D_n\right]_x$$

Surface/Volume ratio (SV) was calculated following the equation:

$$SV\ (cm) = \frac{\dfrac{\pi}{4}\sum_{n=1}^{Z}D_n L_n}{\pi\sum_{n=1}^{Z}D_n L_n}$$

Where, L is the length of individual vessel, D the diameter of the individual vessels, A the area of observation, Z the total number of vessels, and G the number of observed areas.

Values were acquired using an image processing system (National Institutes of Health Image 1.62) [25, 117].

Red blood cell velocity (V$_{RBC}$) was determined using a two-slit method (Exbem 3. Pixlock e.k./ Münster, Germany) and image processing system.

To calculate V_{mean} a correcting factor α [118] was employed which considers that due to the Fahreus Lindquest effect, blood flow velocity is reduced near to the vessel wall and considers laminar flow in vessels. V_{mean} being the mean blood flow velocity where:

$$V_{mean} \, (cm/s) = V_{RBC}/\alpha$$

$\alpha =$ 1.3 for blood vessels < 10 μm;

linear extrapolation 1.3 < α < 1.6 for blood vessels > 10 μm and < 15 μm;

and α = 1.6 m for blood vessels > 15 μm

The blood flow rate (BFR) of individual vessels was calculated as follows:

$$BFR \, (\mu m^3/s) = \pi/4 \; x \; V_{mean} \; x \; D^2$$

3.3.4. Leukocyte-Endothelial-Interaction (LEI) and shear rate

LEI in vessels were visualized *in vivo* after i.v. injection of a 20 µl bolus of 0.1% rhodamine-6G in 0.9 % saline. Images of leukocytes were recorded for a period of 30 seconds (Figure 6). The quantity of rolling (Nr), defined as leukocytes with a velocity < 50% V_{mean}, adhering (Na) leukocytes, defined as cells that adhere during the 30 seconds and the total flux of cells (Nt) along a 100 µm straight vessel segment were documented.

Measurements were equally repeated 4 times in defined areas until data was acquired for 5 fields spread about the chamber so that a mean could be calculated (Figure 5).

The ratio between rolling cells and total flux (Rolling count), density of adhering leukocytes (Adhesion density), leukocyte flux and shear rate [14] for each vessel was calculated with the following equations:

Rolling count (%) = 100 x Nr / Nt

adhesion density (cells/mm^2) = 10^6 x Na / (π x D x 100)

shear rate (µm/s) = 8 x V_{mean} / D,

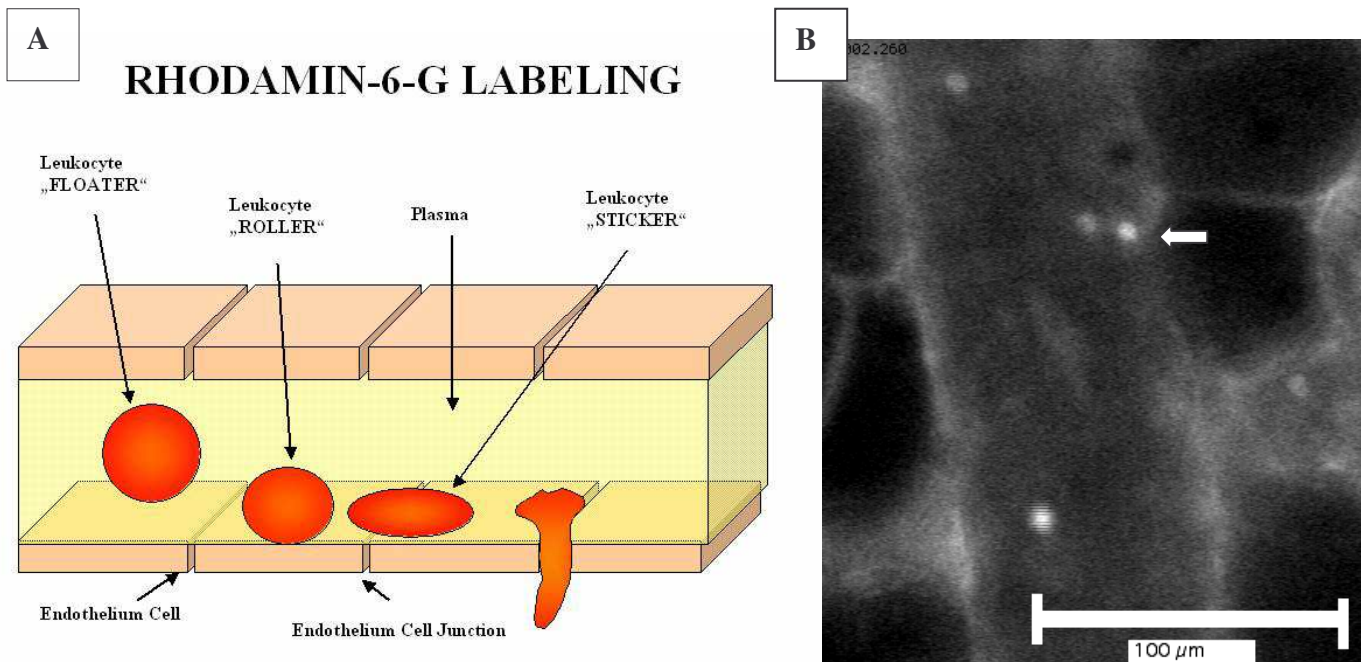leukocyte flux (cells/mm^2 x s) = Nt x 10^6/ π x (D/2)^2 x 30

Figure 6.A. In vivo labeled leucocytes with Rhodamin-6-G. **6.B.** In video sequence their different velocities of leucocytes ($\Rightarrow$) allowing a classification into Rollers, Stickers and floaters. 20x (Zeiss, Oberkochen/Germany).

3.3.5 Vascular permeability (P)

Effective vascular permeability to albumin was measured using tetramethylrhodamine labeled bovine serum albumin (TRITC-BSA, Molecular Probes Eugene, USA) (10 mg/ml, 0.1ml/25g bodyweight). After injected intravenously, the fluorescence intensity was measured intermittently for 5 seconds, to avoid photo bleaching, every 2 minutes for 20 minutes and recorded digitally (Powerlab/2sp, IP Lab Spectrum for Mac, WissTech, Meßdatenerfasungssysteme, Spechbach/Germany) (Figure 7).

The value of P was calculated as [42, 91, 117, 119]:

$$P \text{ (cm/s)} = (1 - HT)\frac{V}{S}\left[\frac{1}{(I_0 - Ib)}\, x\, \frac{dI}{dt} + \frac{1}{K}\right]$$

I is the average fluorescence intensity of the whole image, I_0 being the value of I immediately after filling of all vessels by TRITC-BSA and I_b representing the background fluorescence intensity. V and S are defined as the total volume and surface area of vessels within the tissue volume covered by the surface image, respectively. The average heamatocrit (HT) of vessels is assumed to be equal to 19% [120]. The time constant of BSA plasma clearance (K) is 9.1 x 10^3 s [119]. Rhodamin will diffuse out of the vessel, dependent on the pore cut off size of the endothelium, producing an increase of fluorescence intensity per area.
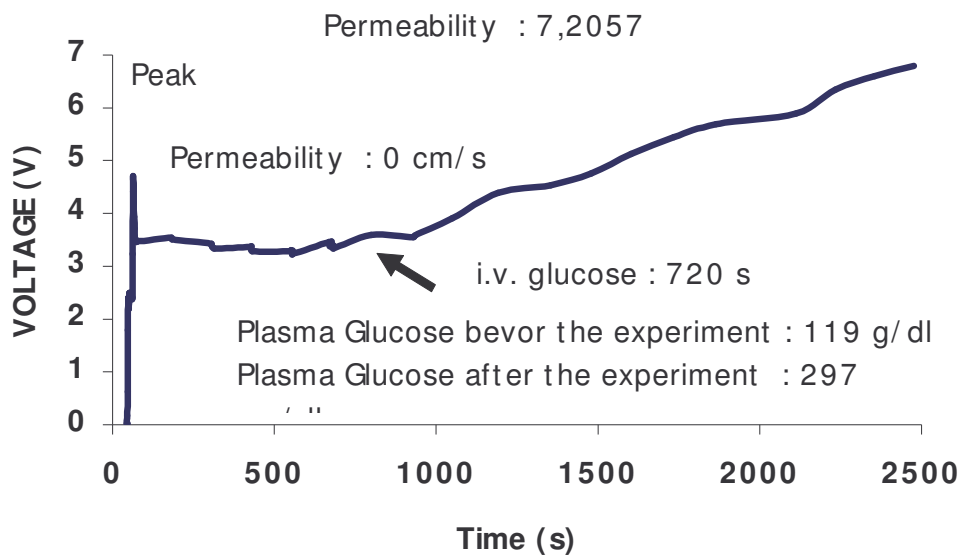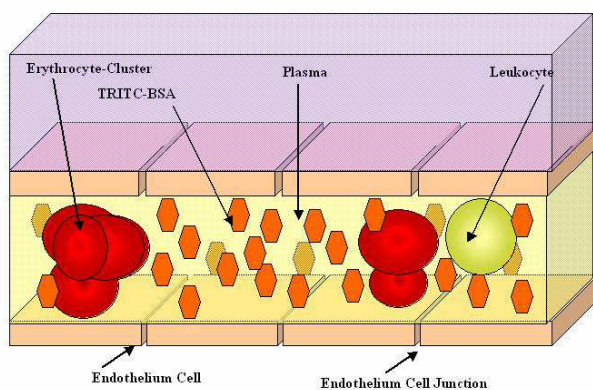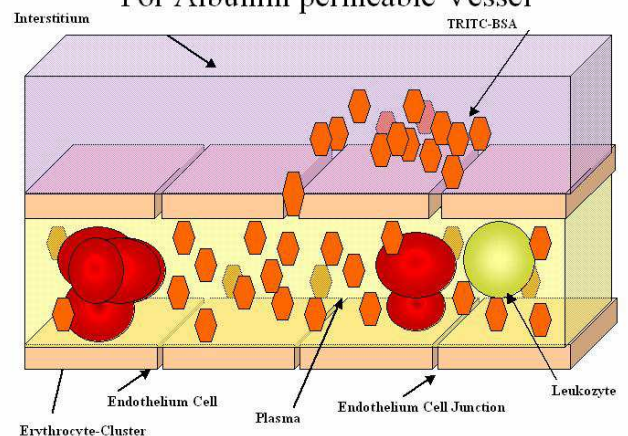
Figure 7.A. An increase of intensity measured implicating an increase of permeability after iv. administration of glucose. Fluorescent intensity I (V) of extravasating fluorochrom plotted against time (s) for measurements of microvascular permeability. Permeability is expressed as a positive inclination. **7.B and 7.C.** Rhodamin BSA diffuses through the vessel wall if an endothelial dysfunction is present.

3.3.6 Intravenous administration and topical application of Glucose, Insulin, HDL and TRL

To analyze the immediate effect that glucose, insulin, HDL and TRL have on the vasculature, various quantities of these substances were administrated systemically during the measurement of permeability. For the topical application we removed carefully the glass cover-slip applied a drop of insulin topically into the chamber and covered the chamber with a new glass cover-slip.

For these experiments we used 12 week old male control littermates. A permeability measurement was performed over a period of 20 minutes as described previously on page 37 followed by a an application of NaCl with the identical volume load of the tested substances, so that a evaluation of the mechanical and haemodynamical component of the administration forms could be made, prior to the administration of these substances (Figure 7A).

Glucose concentrations applied in the first group were equal to those used for the GTT (0.1mg/g bodyweight). In the second group higher doses where applied (0.2mg/g bodyweight) using the same solution (100mg glucose/1ml PBS; 0.6 M). Insulin concentration for the i.v. approach were equal to the concentration (1U/kg) used for i.v. insulin tolerance test.

HDL and TRL concentrations that were chosen, laid under the plasma value that were found in 12 week old UCP1/DTA mice and were chosen relatively low due the mouse intense lipid isolation procedure.

3.4 Statistical Analysis

All results are presented as mean ± standard error of the mean (SEM). To compare the results of the two experimental groups Mann-Whitney U test for unpaired nonparametric samples were performed using StatView (Abacus, Berkeley/CA). Correlations were determined using Spearman-Rank-Correlation test. Statistical significance was based on p values < 5%.

4. Results

4.1 Metabolic Parameters

4.1.1 Body Temperature

Mean body temperature (Figure 8.) of UCP1/DTA mice was significantly lower after overnight fast (37.56 ± 0.24 °C; n=13; p<0.05) compared to controls (38.13 ± 0.53 °C; n=44).

After chamber implantation mean body temperature continued to be significantly lower (day 3: -1.07°C; 36.82 ± 0.16 °C; n=13; p<0.001; day 6: 37.34 ± 0.19 °C; n=18; p<0.005; day 9: 37.3 ± 0.29°C; n=18; p<0.005) then that of controls (day 3: 37.89 ± 0.53 °C; n=35; day 6: 38.08 ± 0.57°C; n=39; day 9: 38.20 ± 0.5°C; n=28), whereas there was a significant drop in body temperature at the third day in UCP1/DTA mice (-0.68°C; p<0.05), with UCP1/DTA only partially recovering the temperature loss (gain from day 3 till 9=0.47°C) in the following days. Control mice suffering a minor non significant temperature drop (-0.24°C), recover completely at the ninth day reaching mean temperature values not differing from those seen prior to chamber implantation.
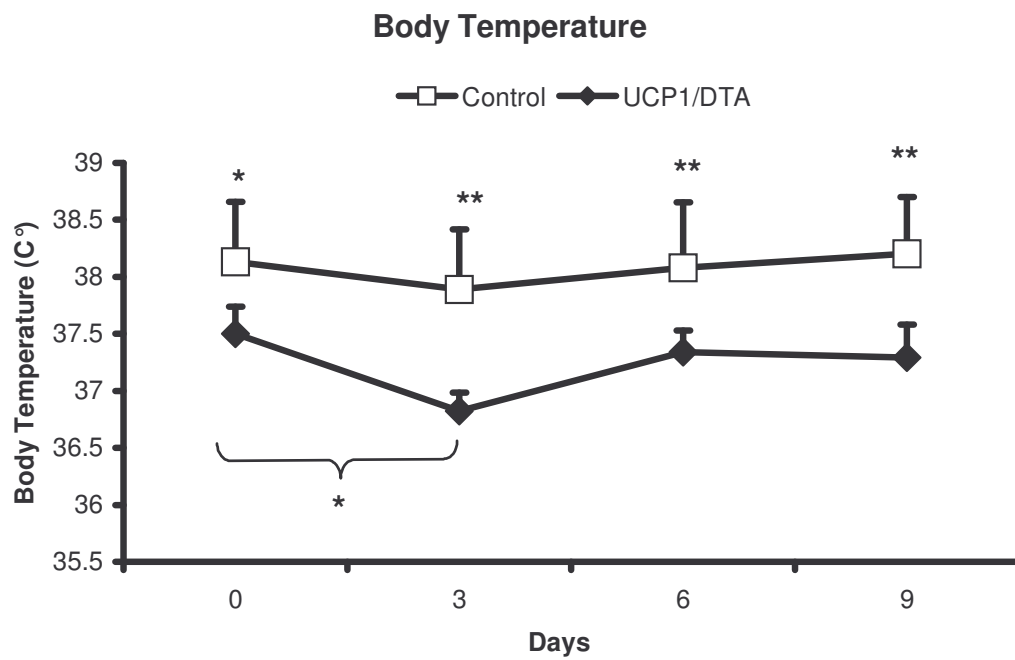
Figure 8. Mean body temperature of UCP1/DTA (day 0 n=13; day 3 n=13; day 6 n=18; day 9 n=18) mice and controls (day 0 n=44; day 3 n=35; day 6 n=39; day 9 n=28) was measured on day 0, 3, 6 and 9 after dorsal skin-fold chamber preparation. Values are presented as mean ± SEM (*p<0.05, **p<0.005).

4.1.2 Bodyweight

Bodyweight of UCP1/DTA mice was at the age of twelve weeks significantly higher (+ 34.27%; 35.64 ± 1.4 g; n=22; $p < 0.0001$) then that of control animals (26.54 ± 3.74 g; n=48) (Figure 9). After chamber implantation the loss of body weight (UCP1/DTA: -16.54%; 5.89 g; controls: -6.35%; 1.69 g) in UCP1/DTA mice and in controls, differed significantly between the groups ($p < 0.01$). Values stayed stabile in both experimental groups on day 3 (UCP1/DTA: 29.74 ± 1.49 g; n=17; $p < 0.05$; controls: 24.86 ± 3.30 g; n=36) and day 6 (UCP1/DTA: 29.9 ± 1.50 g; $p < 0.005$; n=20; controls: 24.94 ± 3.47 g; n=42). A further significant drop followed in UCP1/DTA mice on day 9 (-4.91%; 1.47 g; $p < 0.05$) leading to comparable bodyweight between UCP1/DTA (28.43 ± 1.57 g; n=19) and controls (26.1 ± 3.09 g; n=30).
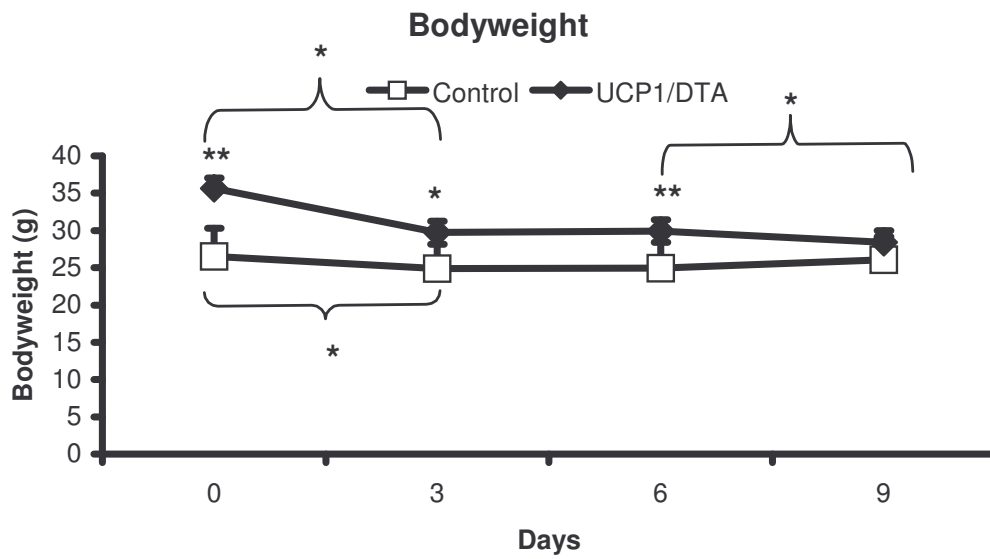
Figure 9. Mean bodyweight of UCP1/DTA (day 0: n=22; day 3: n=17; day 6: n=20; day 9: n=19) mice and controls (day 0: n=48; day 3: n=36; day 6: n=42; day 9: n=30) was measured on day 0, 3, 6 and 9 after dorsal skin-fold chamber preparation. Values are presented as mean $\pm$ SEM (*p<0.05, **p<0.005).

4.1.3 Blood Glucose

Neither fasting glucose values on day 0 (UCP1/DTA: 112.17 ± 8.51 mg/dl; n=18) (control: 108.87 ± 30.97 mg/dl; n=47) nor blood glucose values on day 3, 6 and 9 (Figure 10) showed a significant difference between UCP1/DTA mice (day 3: 99.33 ± 9.19 mg/dl; n=15; day 6: 118.45 ± 7.05 mg/dl; n=20; day 9: 105.82 ± 9.43 mg/dl; n=11) and their control littermates (day 3: 100.85 ± 20.13 mg/dl; n=26; day 6: 114.45 ± 29.70 mg/dl; n=38; day 9: 113.33 ± 26.72 mg/dl; n=30). These data corroborate that at this stage UCP1/DTA mice were not diabetic.
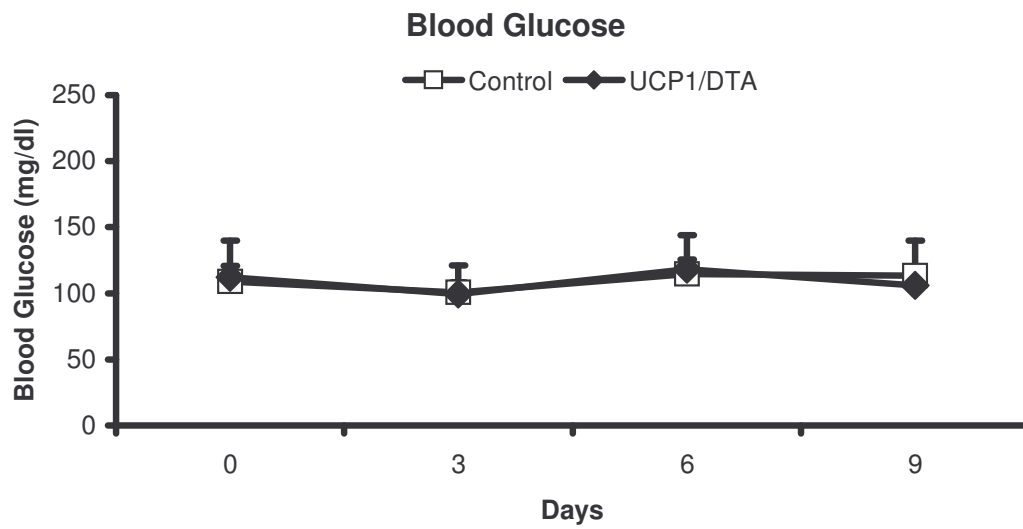
Blood Glucose

Figure 10. Blood glucose levels in UCP1/DTA mice (day 0: n=18; day 3: n=15; day 6: n=20; day 9: n=11) and controls (day 0: n=47; day 3: n=26; day 6: n=38; day 9: n=30) were measured on day 0, 3, 6 and 9 after dorsal skin-fold chamber preparation. Blood glucose levels on day 0 were measured after overnight fast. Values are presented as mean $\pm$ SEM (*p<0.05, **p<0.005).

4.1.4 Glucose Tolerance Test (G-T-T)

UCP1/DTA mice showed a pathological glucose tolerance (Figure 11) with unaltered fasting glucose values. Maximum blood glucose levels in UCP1/DTA mice were +27.13% higher (204.13 $\pm$ 21.26 mg/dl; n=16) then that of controls (160.56 $\pm$ 39.40 mg/dl; n=32). After continuous increase, maximum levels were reached 60 minutes after the intraperitoneal injection of the glucose solution. On the contrary maximum blood glucose levels in control mice remained at constant levels 15 minutes after injection. Furthermore blood glucose values after 2 hours still showed significant higher values (+32.28%) in UCP1/DTA mice (168.5 $\pm$ 20.16 mg/dl; n=14; p<0.05) compared to controls (119.4 $\pm$ 29.69 mg/dl; n=25), representing an increase of +50.22 % (p<0.05) compared to fasting values. In contrast controls only showed a slight increase of –9.67% compared to initial blood glucose, not being significant.
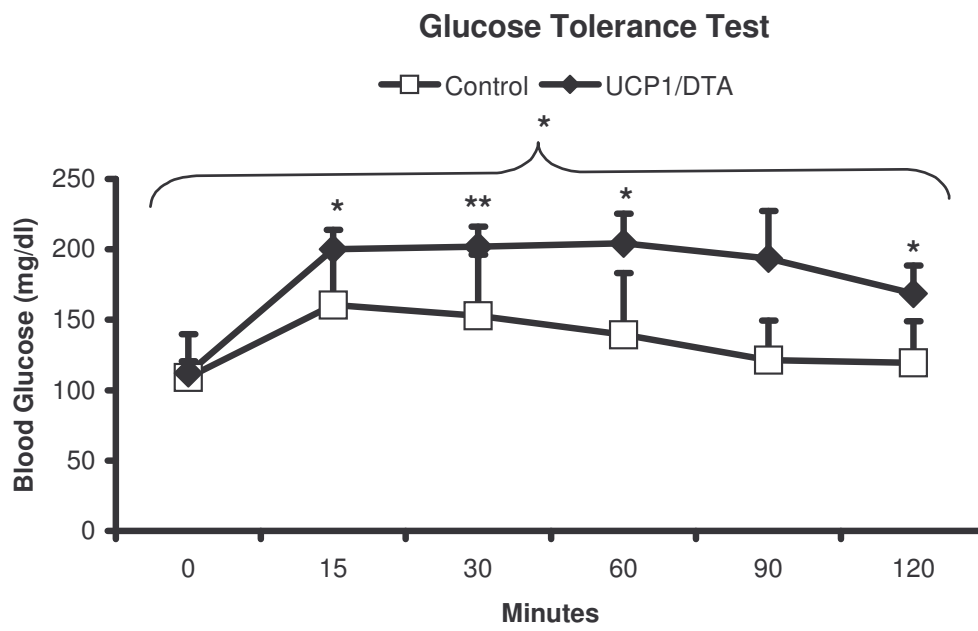
Glucose Tolerance Test

Figure 11. Glucose tolerance test performed on UCP1/DTA (n=18) mice and controls (n=47) prior to dorsal skin-fold chamber preparation after overnight fast. Values are presented as mean ± SEM (*$p<0.05$, **$p<0.005$).

4.1.5 Serum Lipid Profile

Serum cholesterol levels after overnight fast were significantly increased (+33.98 %; 50.55 mg/dl) in male UCP1/DTA (199.32 ± 6.59 mg/dl; n=10; p<0.005) mice when compared to controls (41.6 ± 13.47 mg/d) (Figure 12). Furthermore triglyceride values of UCP1/DTA (300.81 ± 10.84 mg/dl; n=10; p<0.0005) were significantly elevated (+97.37%; 148.40 mg/dl) compared to controls (152.41 ± 16.1 mg/dl; n=10) (Figure 13). Free fatty acids showed no significant difference in UCP1/DTA mice (0.79 ± 0.09 mmol/ml; n=5) compared to controls (1.09 ± 0.13 mmol/ml; n = 5)(Figure 14).
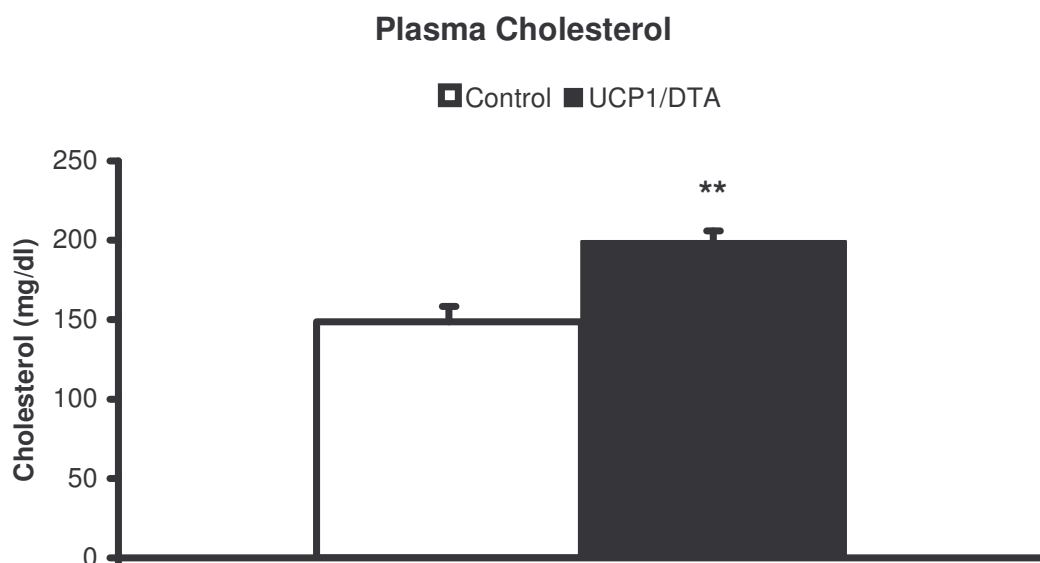

Figure 12. Plasma cholesterol of UCP1/DTA (n=10) mice and controls (n=10). Values are presented as mean ± SEM (*p<0.05, **p<0.005).
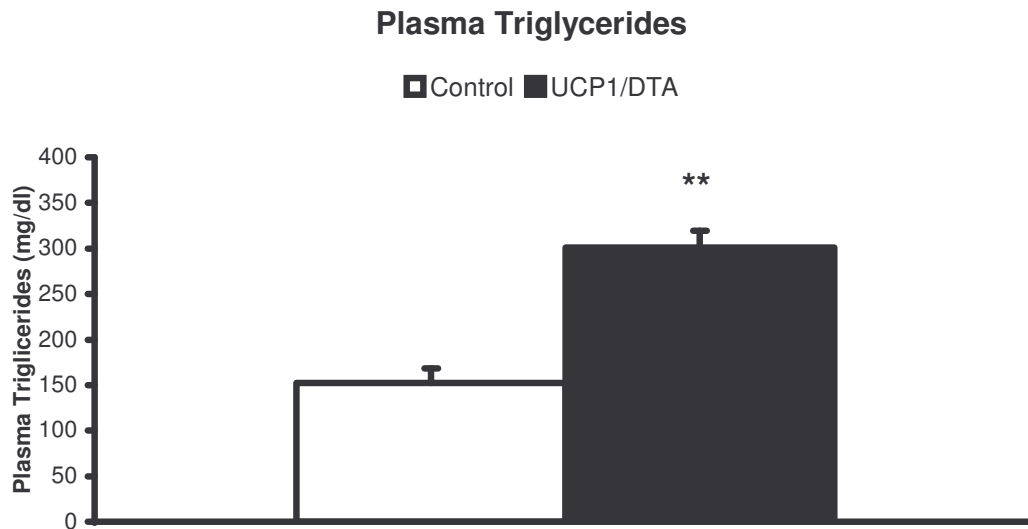
Plasma Triglycerides

Figure 13. Plasma triglycerides of UCP1/DTA (n=10) mice and controls (n=10).
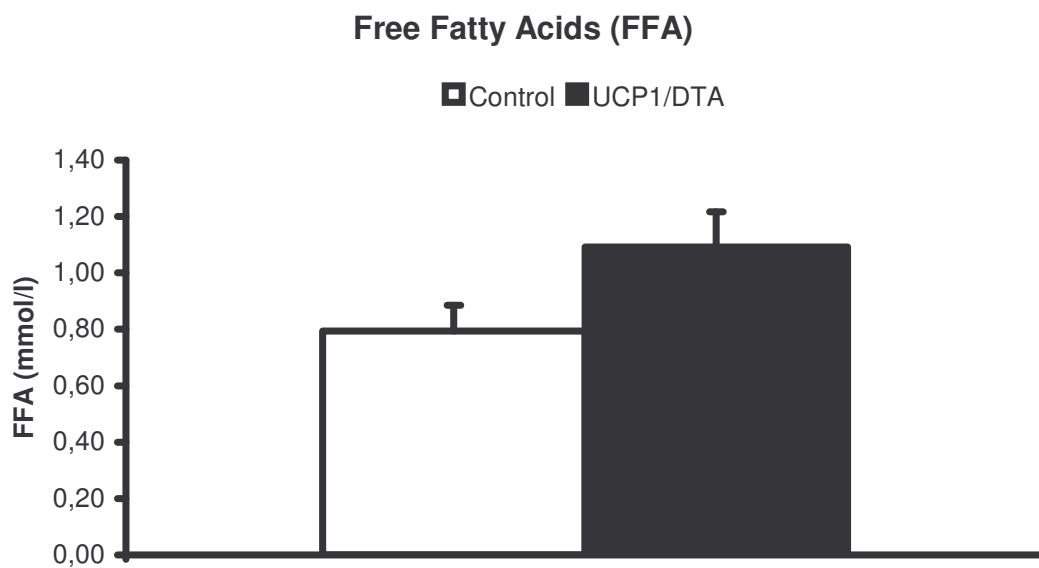
Free Fatty Acids (FFA)

Figure 14. Free Fatty Acids in plasma of UCP1/DTA (n=5) mice and controls (n=5). Values are presented as mean $\pm$ SEM (*p<0.05, **p<0.005).

Up to this point the lipid profile of UCP1/DTA mice had not been analysed. Our results showed surprisingly that in the HDL, LDL, chilomicron and VLDL fractions UCP1/DTA mice have a higher concentration of cholesterol rich lipoproteins (Figures 15 and 17). On the other hand, the FLPC of triglycerides (Figures 16 and 18) showed a pronounced difference in the chilomicron and VDL fractions.

Furthermore these analysis were performed to identified the fraction required for the performed stimulation test as described more detailed on

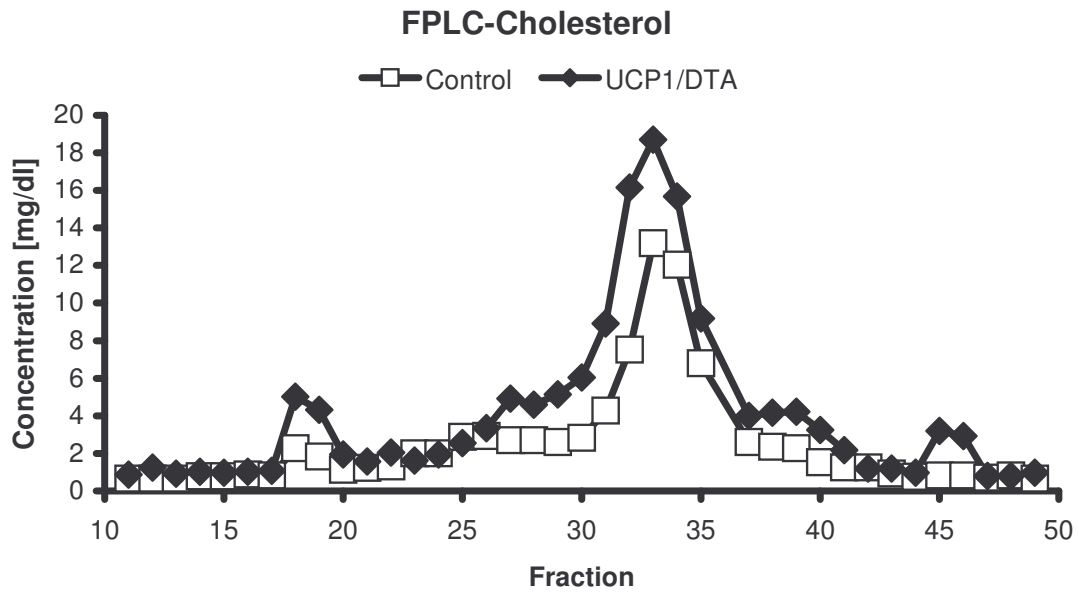**FPLC-Cholesterol**

Figure 15. FLPC of cholesterol (n=5).

FPLC-Triglicerides
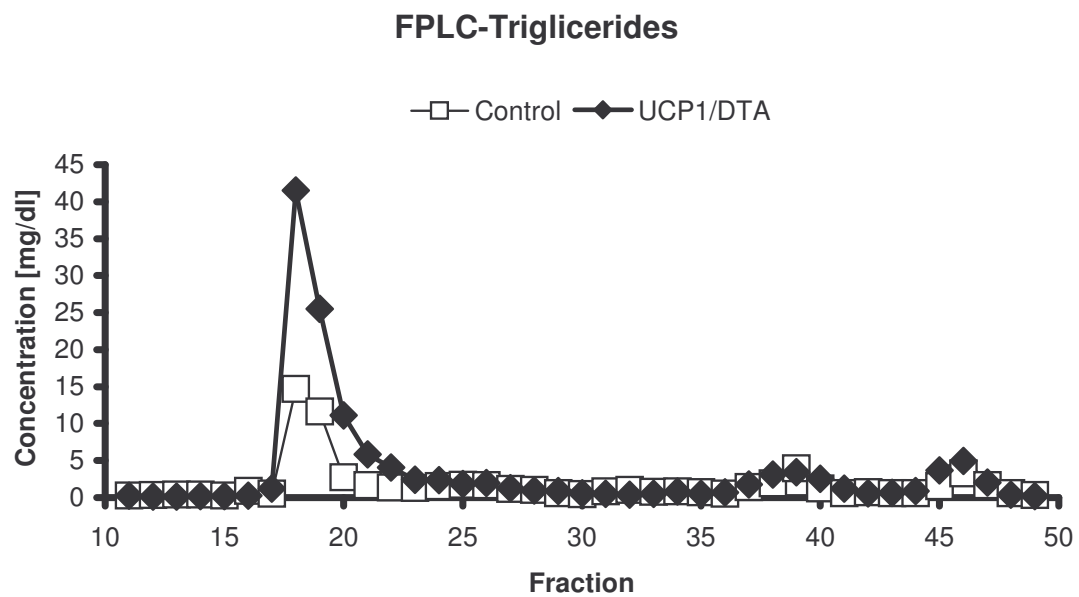
Figure 16. FLPC of triglycerides (n=5).
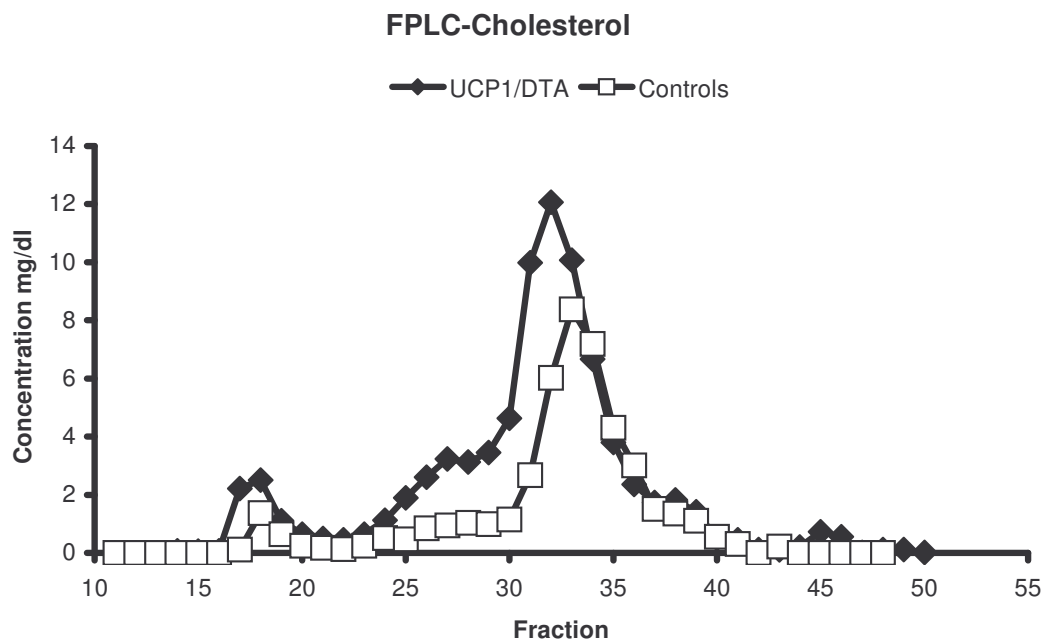
FPLC-Cholesterol

Figure 17. Repeated FPLC of cholesterol with different mice (n=5).
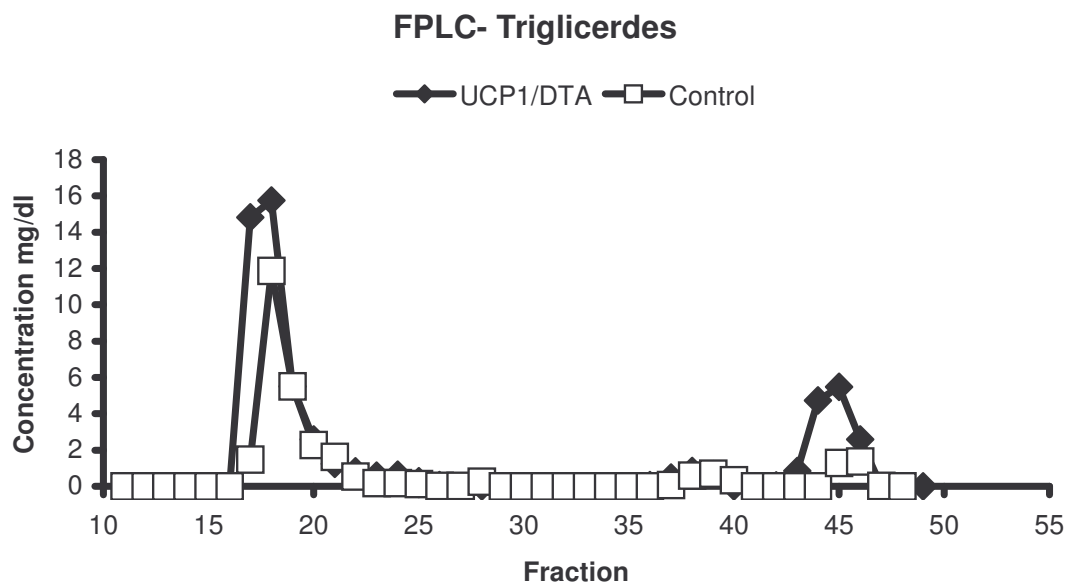
FPLC- Triglicerdes

Figure 18. Repeated FPLC of triglyerides with different mice (n=5).

4.2 Microvascular Parameters

4.2.1 Morphological Microcirculatory Parameters

4.2.1.1 Functional Vessel Density, Diameter, and Surface-Volume Ratio (S/V)

While the functional vascular density (Figure 19) differed significantly (-17.74%; p<0.05) between UCP1/DTA mice (274.99 ± 15.36 cm/cm^2; n=7) and control mice (334.29 ± 12.29 cm/cm2; n=17) on day 6, the significant difference decreased to a trend on day 9, possibly due to increased SEM values in UCP!/DTA mice.(UCP1/DTA: 258.61 ± 29.51 cm/cm2; n=7; control: 304.28± 16.32 cm/cm2; n=14).

Furthermore we observed on both days a significant increase of functional vessel diameter (Figure 20) in UCP1/DTA (day 6: +35.25%; p<0.005; 14.35 ± 1.23 µm; n=7; day 9: +27.48%; p<0.05; 13.64 ± 0.81 µm; n=7) mice versus control mice (day 6: 10.61 ± 0.36 µm; n=17; day 9: 10.7 ± 0.69 µm; n=14).

Functional Vessel Density (VD)

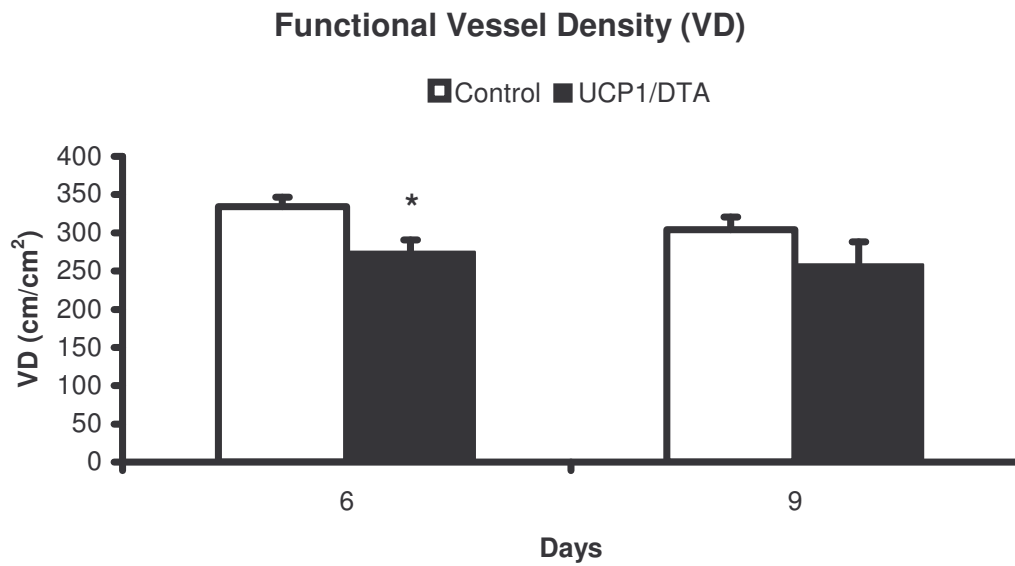**Figure 19.** Functional vascular density on day 6 and 9 after chamber implantation in UCP1/DTA mice (day 6: n=7; day 9: n=7) and controls (day 6: n=17; day 9: n=14).

Functional Vessel Diameter
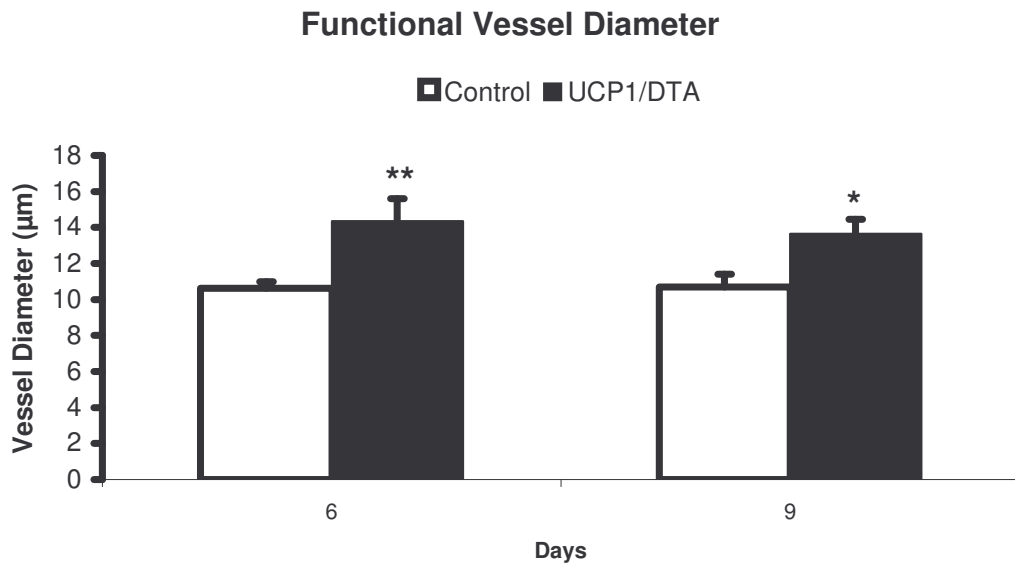
Figure 20. Functional vascular diameter on day 6 and 9 in UCP1/DTA mice (day 6: n=7; day 9: n=7) and controls (day 6: n=17; day 9: n=14). Values are presented as mean ± SEM (*p<0.05, **p<0.005).

Also the surface-volume (Figure 21) was significantly lower in UCP1/DTA mice (day 6: -22.77 %; 0.20 ± 0.02µm; n=7; p<0,005; day 9: -36.73 %; 0.1740 ± 0.01µm; n=7; p<0.05;) compared to controls (day 6: 0.26 ± 0.01 µm; n=15; day 9: 0.28 ± 0.03 µm; n=11).

Surface/Volume (SV)
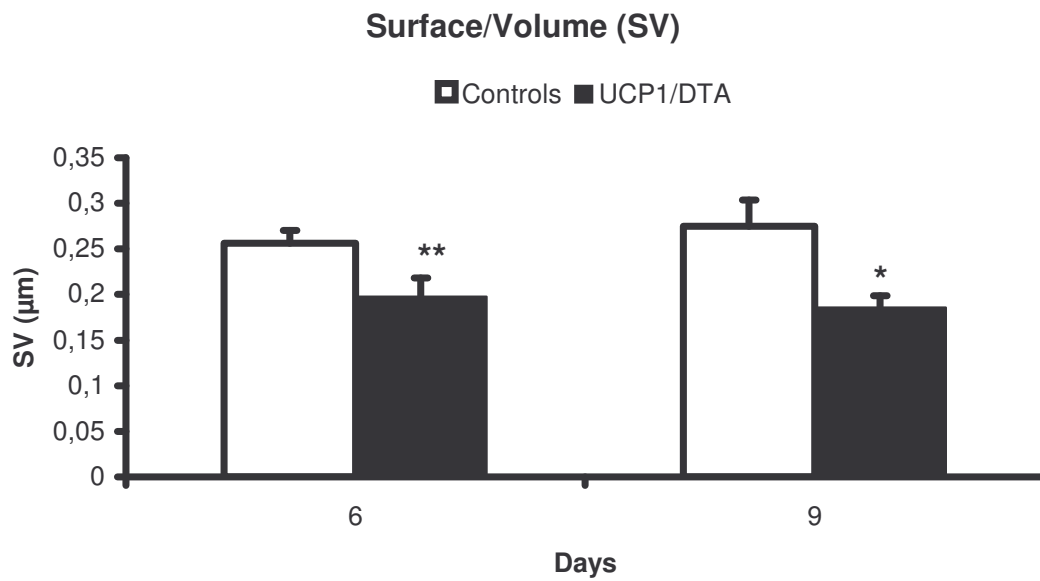
□Controls ■UCP1/DTA

Figure 21. Surface-volume in UCP1/DTA mice (day 6: n=7; day 9: n=7) compared to controls (day 6: n=15; day 9: n=11). Values are presented as mean ± SEM (*p<0.05, **p<0.005).

The vessel diameter distribution (Figures 22 and 23) in UCP1/DTA mice showed that the diameter peak of UCP1/DTA on day 6 (82.81%) of total count of vessel with diameters between 0-18μm) was significantly lower compared with the diameter peak of control animals (90.34% of total count vessel with diameters between 0-18μm). This significant reduction of small vessels in UCP1/DTA mice was less pronounced on day 9 due to an isolated increase in 9 μm vessels in UCP1/DTA mice. However the difference in vessel diameter distribution was still significant. Vessel diameter peak laid in UCP1/DTA at 8μm on day 6 and at 8μm on day 9, in contrast to the diameter peak at 6μm on day 6 and at 7μm on day 9 of control animals, demonstrating that increase of vessel diameter being mainly caused by a relative reduction of small vessels in UCP1/DTA mice.

Vessel Count plotted against Vessel Diameter Day 6
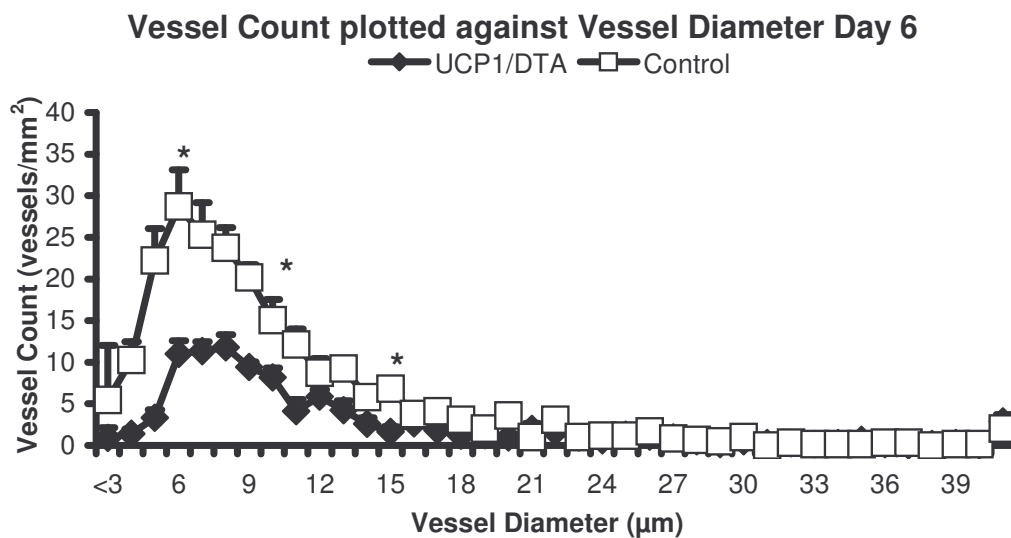
Figure 22. Vessel diameter distribution in UCP1/DTA mice on day 6 (n=7) compared to controls (n=17).

Vessel Count plotted against Vessel Diameter on Day
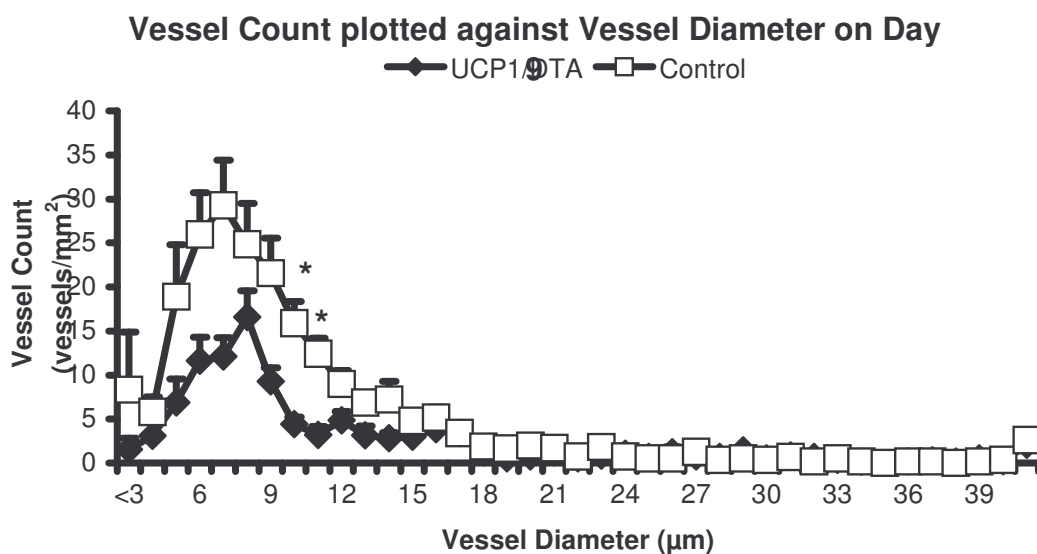
Figure 23. Vessel diameter distribution in UCP1/DTA mice on day 9 (n=6) compared to controls (n=12). Values are presented as mean ± SEM (*p<0.05, **p<0.005).

4.2.2 Functional Microcirculatory Parameters

4.2.2.1 Red Blood Cell Velocity and Blood Flow Rate (BFR)

UCP1/DTA mice (day 6: 161.12 $\pm$ 33.20 µm/s; n=7; day 9: 184.68 $\pm$ 28.71 µm/s; n=8) showed no significant difference concerning mean red blood cell velocity (Figure 24) on day 6 and 9 compared to that of controls (day 6: 244.33 $\pm$ 28.03 µm/s; n=17; day 9: 290.88 $\pm$ 47.83 µm/s; n=2).

Furthermore no alterations were observed in the blood flow rate (Figure 25) of UCP1/DTA mice (day 6: $5.71 \times 10^{-05} \pm 7.61 \times 10^{-06}$ µm^3/s; n=7; day 9: $7.68 \times 10^{-05} \pm 2.8E^{-05}$ µm^3/s; n=8) when compared to controls (day 6: $5.09 \times 10^{-05} \pm 7.25 \times 10^{-06}$ µm/s; n=17; day 9: $4.84E-05 \pm 1.15 \times 10^{-05}$ µm^3/s; n=12).

Mean Red Blood Cell Velocity (Vmean)

□Control ■UCP1/DTA

Figure 24. Mean red blood cell velocity in UCP1/DTA mice (day 6: n=7; day 9: n=8) compared to controls (day 6: n=15; day 9: n=12).

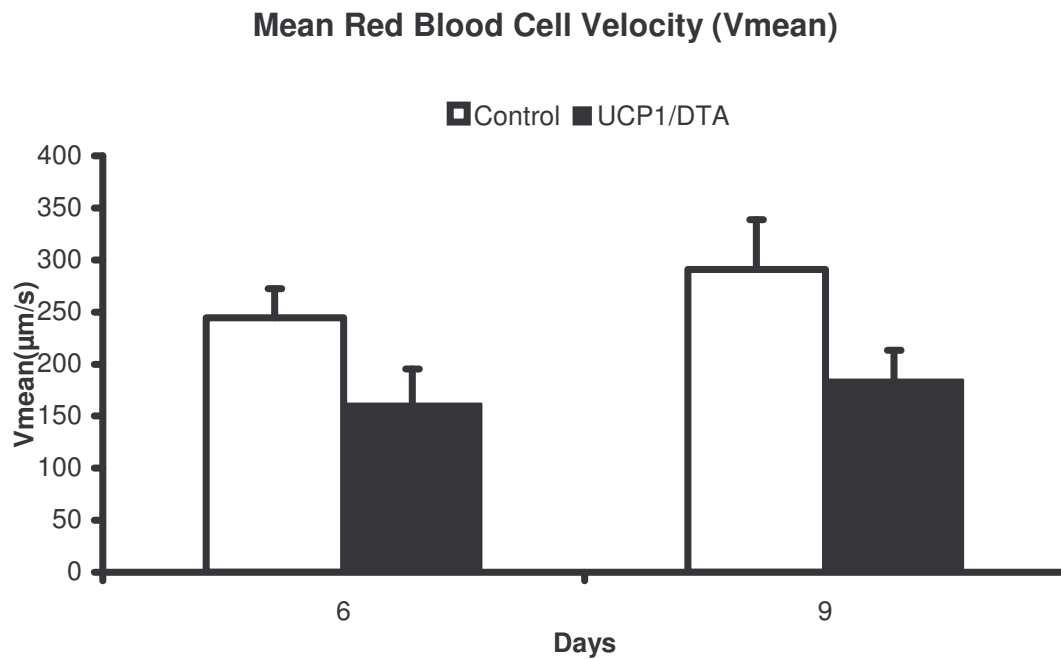**Blood Flow Rate (BFR)**

□Control ■UCP1/DTA

Figure 25. Blood flow rate in UCP1/DTA mice (day 6: n=7; day 9: n=8) compared to controls (day 6: n=15; day 9: n=12). Values are presented as mean ± SEM (*p<0.05, **p<0.005).

4.2.2.2 Leukocyte-Endothelium-Interactions (LEI) and Shear Rate

UCP1/DTA mice and controls showed differences in LEI, represented by a significant increase of leukocyte cell adhesion in UCP1/DTA mice (mean 346.11 $\pm$ 79.05 cells/mm^2; n=5;p<0,05) compared to the control group (mean 145.67 $\pm$ 41.19 cells/mm^2; n=9) on day 6 (Figure 26). However on day 9 there were no significant differences found concerning leukocyte cell adhesion between UCP1/DTA mice (274.24 $\pm$ 83.50 cells/mm^2; n=5) and controls (205.46 $\pm$ 50.66 cells/mm^2; n=8). The approximation in LEI on day 9 between UCP1/DTA mice and controls was mainly due to a decrease of leukocyte cell adhesion in UCP1/DTA (-20.76%) combined with the increase of cell adhesion in controls (+41.04%) with both changes not being significant.

Furthermore the leukocyte rolling count (Figure 27) was not significantly altered in UCP1/DTA mice (day 6: 18.29 $\pm$ 6.94 %; n=5; day 9: 16.87 $\pm$ 4.92 %; n=5) versus controls (day 6: 26.59 $\pm$ 5.17 %; n=9; day 9: 11.14 $\pm$ 3.56 %; n=8) on both days. Controls however showed a significant decrease of –41.88% (p<0.05) on the ninth day compared to day six concerning the leukocyte rolling count.
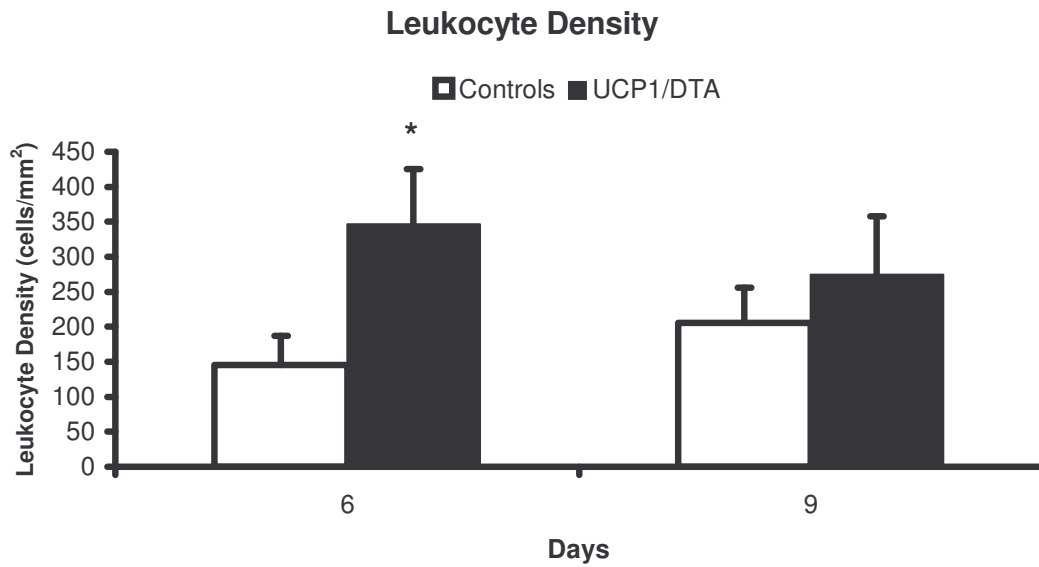
Leukocyte Density

Figure 26. Leukocyte cell density in UCP1/DTA mice (day 6: n=5; day 9: n=5) compared to controls (day 6: n=9; day 9: n=8).
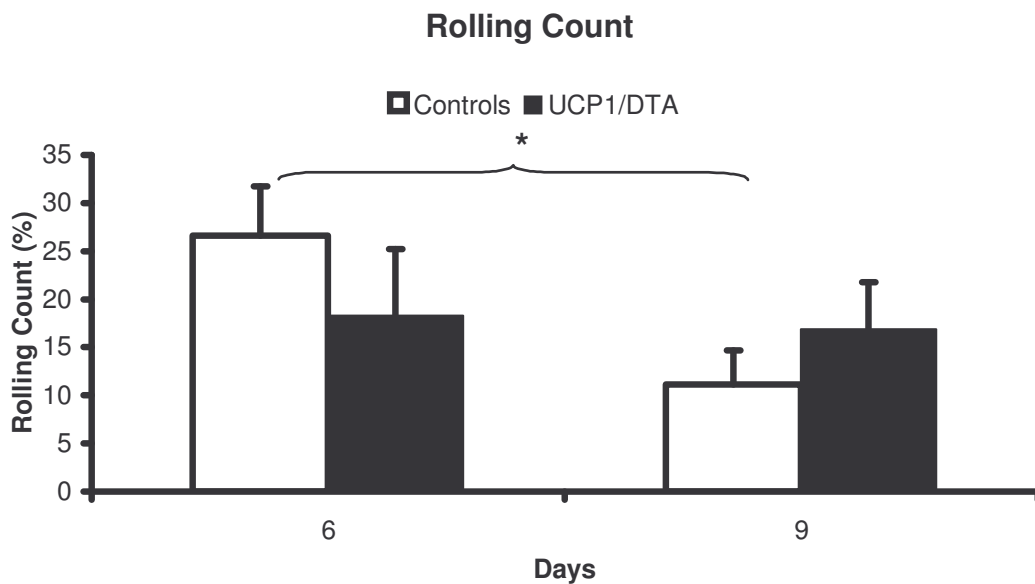
Rolling Count

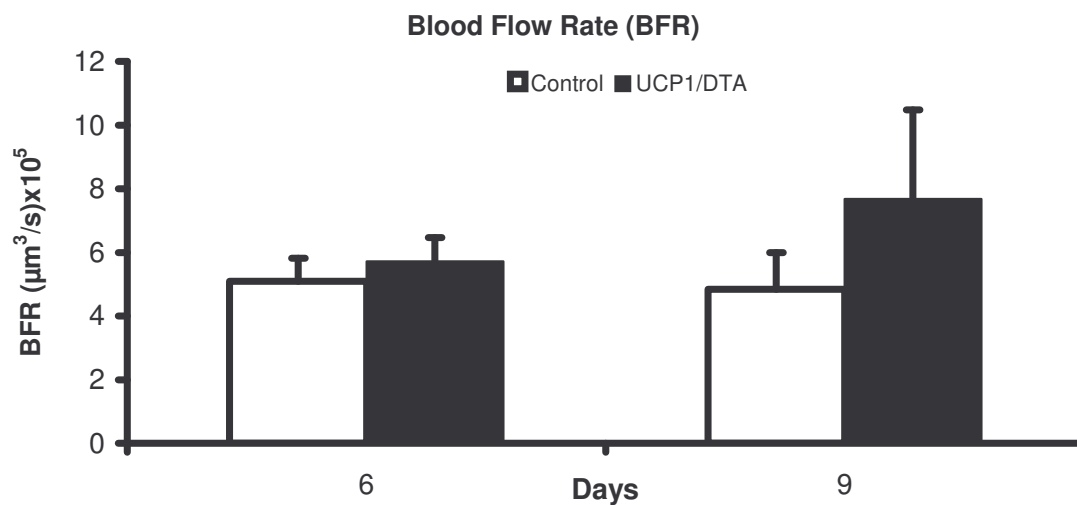**Figure 27.** Leukocyte rolling count in UCP1/DTA mice (day 6: n=5; day 9: n=5) compared to controls (day 6: n=9; day 9: n=8). Values are presented as mean $\pm$ SEM (*p<0.05, **p<0.005).

No significant differences were observed in leukocyte cell flux per cross sectional area (Figure 28) between UCP1/DTA mice (day 6: 3856.32 $\pm$ 818.83 cells/mm^{2}s; n=5; day 9: 10507.40 $\pm$ 2706.23 cells/mm^{2}s; n=5) and controls (day 6: 5098.73 $\pm$ 508.48 cells/mm^{2}s; n=9; day 9: 8161.02 $\pm$ 1999.86 cells/mm^{2}s; n=8). UCP1/DTA mice showed a significant increase of leukocyte cell flux per cross sectional area between day 6 and 9. (UCP1/DTA: +172.47% $p<0.05$; controls: +60.06%; not significant)

Interestingly the shear rate (Figure 29) showed a tendency ($p<0.1$) to lower values (-48.34 % on day 6 and –44.3% on day 9) in UCP1/DTA mice (day 6: 108.20 $\pm$ 29.78 $^{s-1}$; day 9: 120.85 $\pm$ 23.87 $^{s-1}$) compared to control animals (day 6: 209.44 $\pm$ 35.09 $^{s-1}$; day 9: 216.96 $\pm$ 38.87 $^{s-1}$).
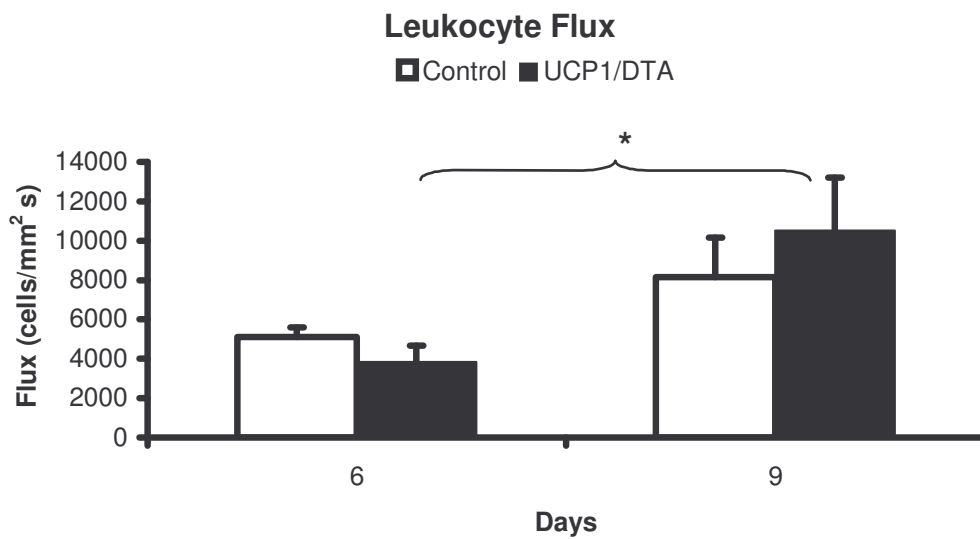
Figure 28. Leukocyte cell flux per cross sectional area in UCP1/DTA mice (day 6: n=5; day 9: n=5) compared to controls (day 6: n=9; day 9: n=8).
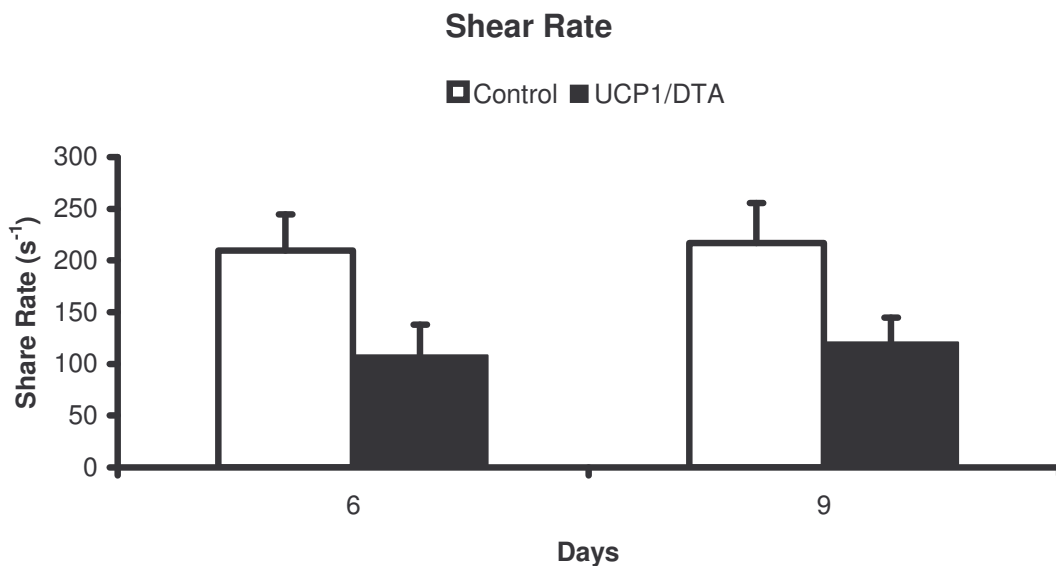
Figure 29. Shear Rate on day 6 and 9 after chamber implantation in UCP1/DTA mice (day 6: n=7; day 9: n=8) and controls (day 6: n=17; day 9: n=12). Values are presented as mean ± SEM (*p<0.05, **p<0.005).

4.2.2.3 Permeability

Significant increase ($p<0.05$) of permeability to albumin (Figure 30) was observed in UCP1/DTA ($1.252 \times 10^{-08} \pm 2.59 \times 10^{-08}$ cm/s; n=6) mice compared to control animals ($6.717 \times 10^{-08} \pm 1.513 \times 10^{-08}$ cm/s; n=17) on day six. However on day 9, the SEM in the UCP1/DTA group ($10.0675 \times 10^{-08} \pm 6.6193 \times 10^{-08}$ cm/s; n=4) increased so that the difference between controls ($6.8244 \times 10^{-08} \pm 2.493 \times 10^{-08}$ cm/s; n=11) and UCP1/DTA mice lost the significant level.
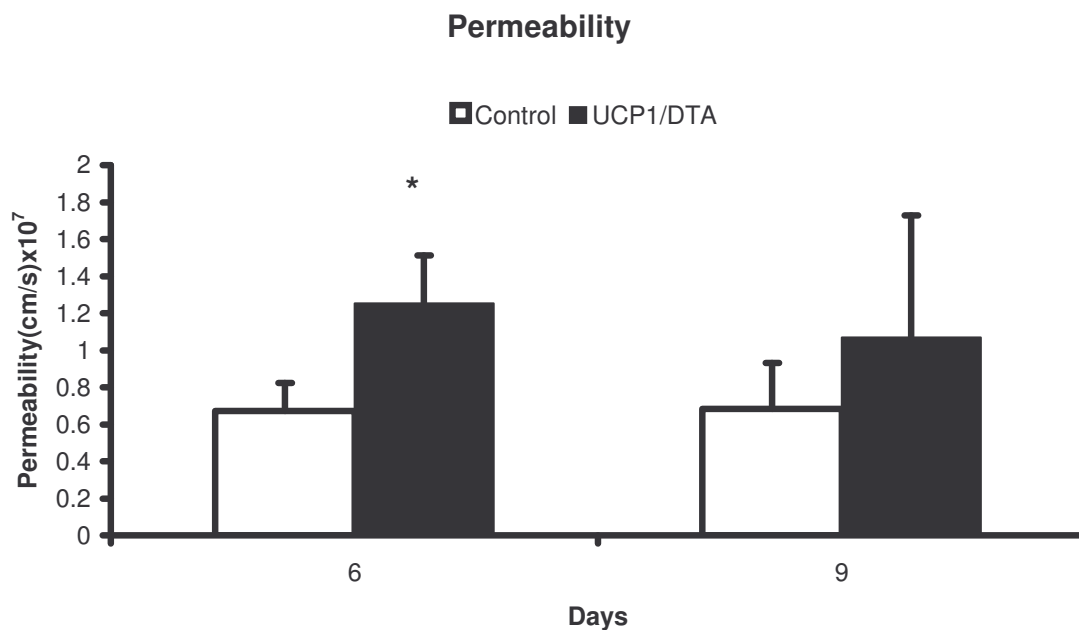
Figure 30. Microvascular Permeability on day 6 and 9 after dorsal skin-fold chamber implantation in UCP1/DTA mice (day 6: n=6; day 9: n=4) and controls (day 6: n=17; day 9: n=11). Values are presented as mean $\pm$ SEM (*$p<0.05$, **$p<0.005$).

4.3 Correlation of Body weight, Body Temperature and Microvascular Parameters

No significant linear correlation was found between weight and measured microvascular parameters when tested independently of group or day.

4.4 Topical and Systemic administration of Insulin, Glucose, HDL and TRL:

4.4.1 Insulin

The experiments to test the effect of topical administration of insulin (Figure 31) demonstrated an increase of vascular permeability from subcutaneous vessels to albumin when as control substance NaCl was administrated ($0.15 \pm 0.07 \times 10^{-4}$%; n=3; p<0.05). When insulin (0,005ml Actrapid) was applied there was a significant increase ($0.47 \pm 0.45 \times 10^{-4}$%; n=3; p<0.05) seen. The increase was even more pronounced ($1.15 \pm 0.35 \times 10^{-4}$%; p<0.005; n=6) when insulin was applied directly into the chamber, without a prior NaCl application as a control substance.

Systemic application of NaCl (Figure 32) had no significant effect on permeability to albumin ($0.05 \pm 0.02 \times 10^{-4}$%; n=6). Administration of equal volumes of insulin (0.001ml/1g Actrapid) did not increase permeability significantly ($0.06 \pm 0.03 \times 10^{-4}$%; n =2).

Topical Insulin 0,05ml
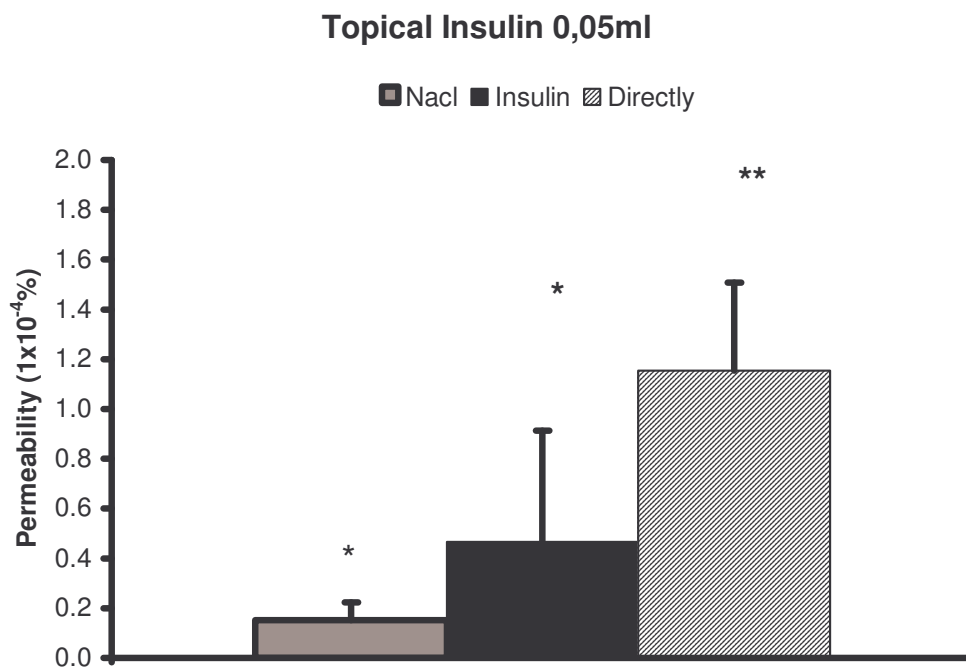
Figure 31. Permeability after topical administration of insulin.
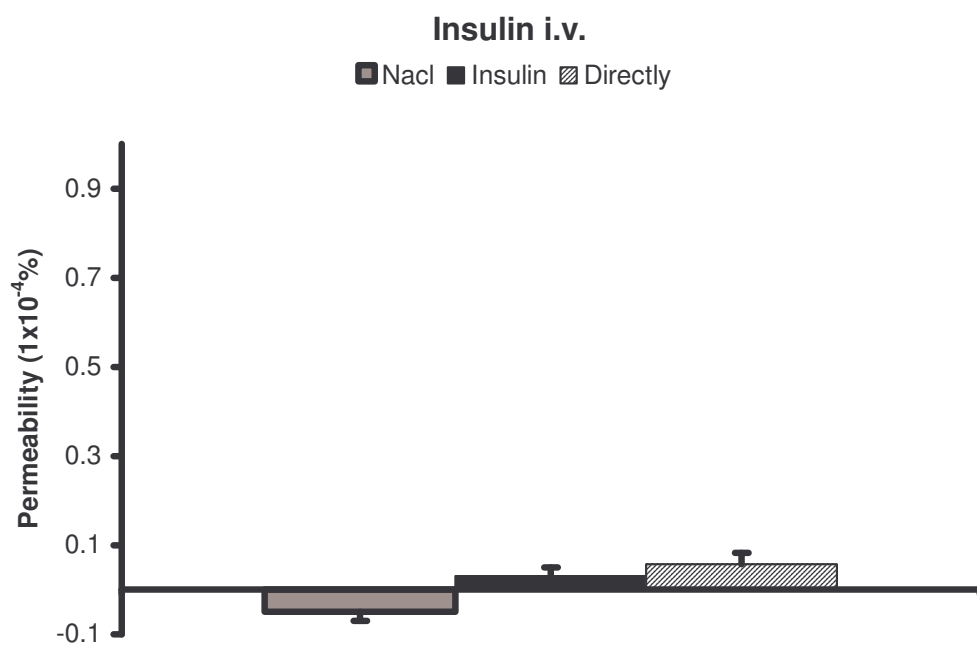
Insulin i.v.

Figure 32. Permeability after systemic administration of insulin.

4.4.2 Glucose

A significant increase of vascular permeability for albumin ($0.12 \pm 0.05 \times 10^{-4}$%; n=5; p<0.05) was observed after systemic administration of glucose (0.01ml/1g body weight of a 100mg/ml glucose solution). Preceding applied NaCl injection showed no significant difference ($0.03 \pm 0.08 \times 10^{-4}$%) (Figure 33).

When higher glucose doses of 0.02mg/g body weight with a higher volume load were applied a significant increase (After NaCl: $0.17 \pm 0,00 \times 10^{-4}$%; n=2; direct: $0.51 \pm 0,27 \times 10^{-4}$%; n=2; p<0,05) of permeability was observed (Figure 34). NaCl repeatedly applied, had no effect on permeability ($-017. \pm 0.00 \times 10^{-4}$%).

Increase of permeability starts immediately after application of the glucose solution. The permeability curve reached a plateau around 30 minutes after application.

Glucose i.v.-1
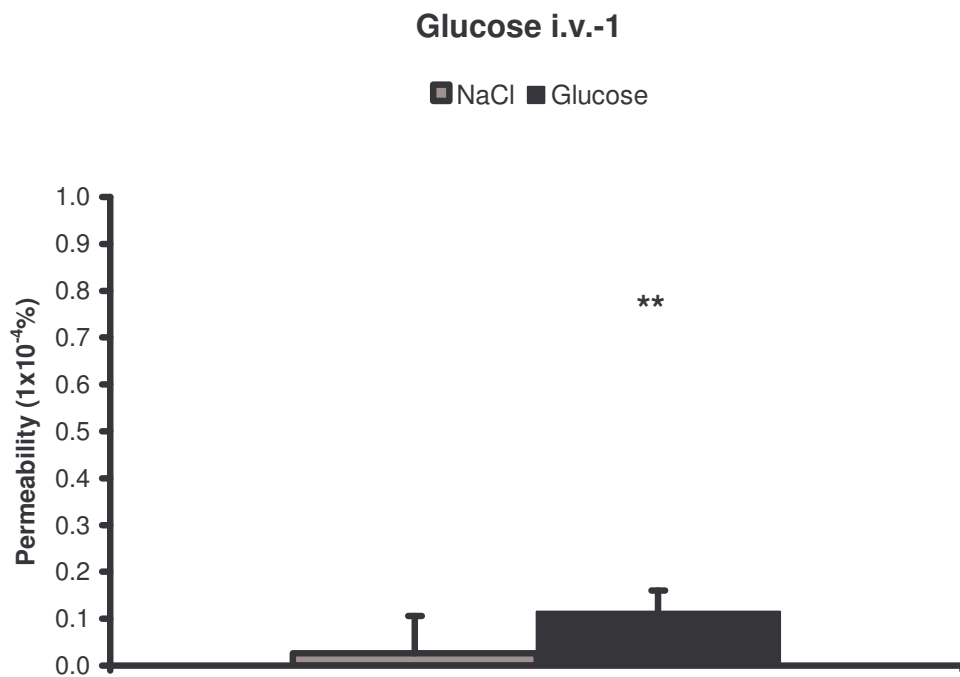
Figure 33. Permeability after administration of 0.01 mg/g (n=4) of glucose.

Glucose iv-2
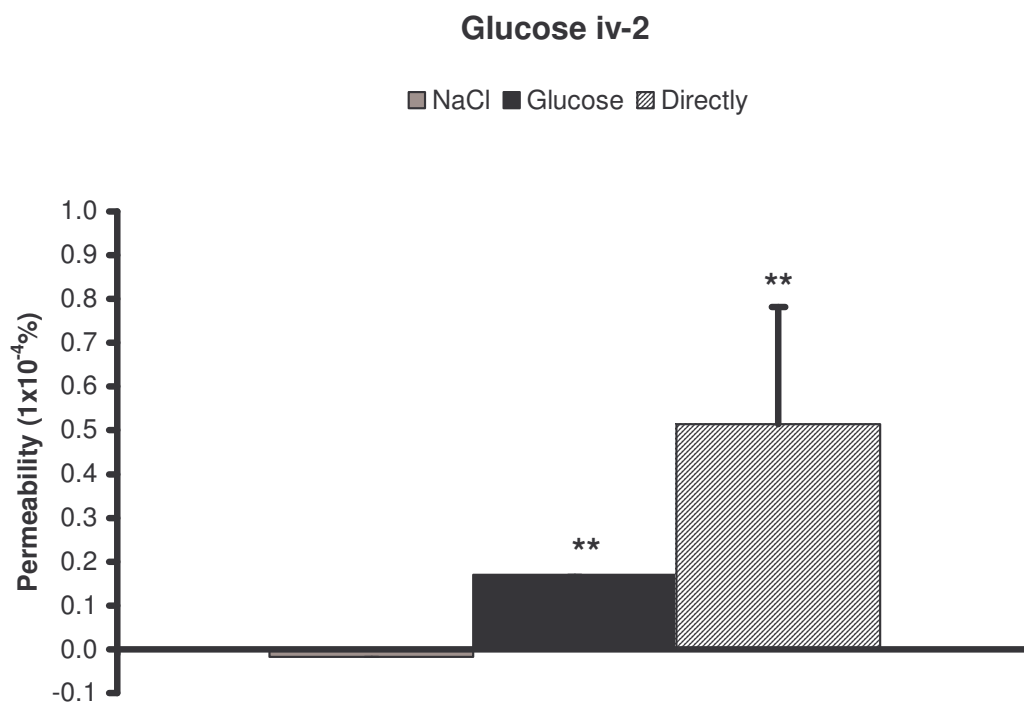
Figure 34. Permeability after administration of 0.02 mg/g (n=2; n=2) of glucose.

4.4.3 TRL

Systemic application (Figure 35) of 0.0387 mg TRL with a volume load of 0.03ml showed no significant increase of vascular permeability (0.16 $\pm$ 0,14x10^{-4}%; n=2). However a higher TRL dose consisting of 0.06256 mg showed a significant increase of 0.03 $\pm$ 0x10^{-4}% (n=4; p<0.05).

Increase of vascular permeability starts immediately after application of TRL. The permeability curve reached a plateau around 30 minutes after application.

TRL i.v.

■ TRL 0.0387mg   ■ TRL 0.06256mg
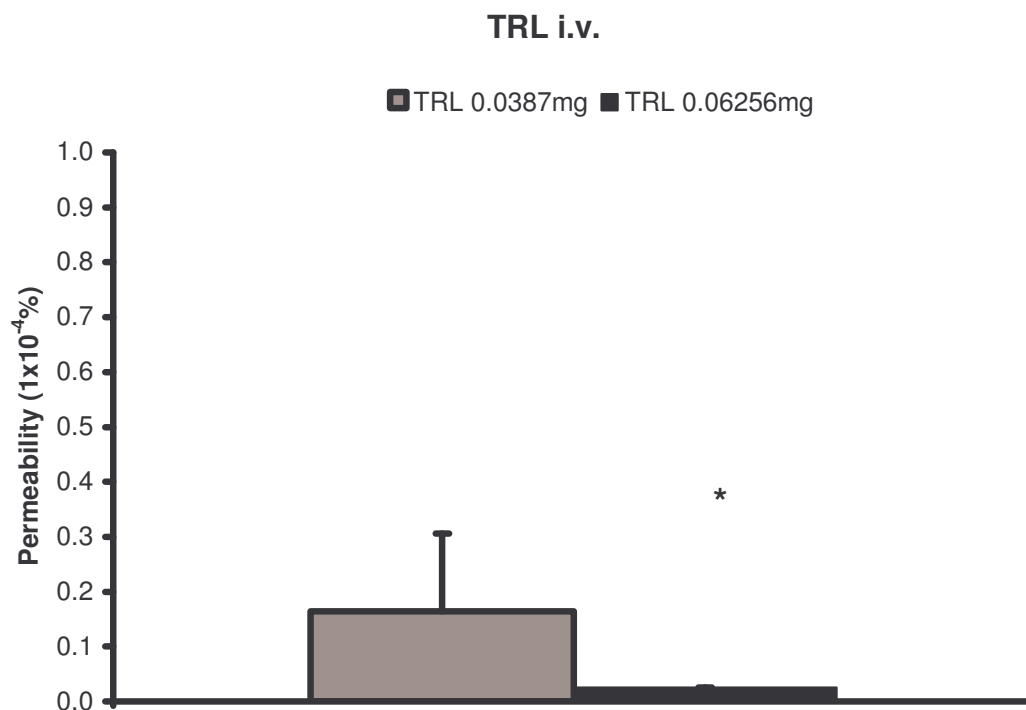
Figure 35. Permeability after administration of 0.0387 mg (n=2) and of 0.06256 mg (n=4) of TRL, respectively.

4.4.4 HDL

Systemic application of 0.0019252 mg HDL with a volume load of 0.02ml showed no significant increase of vascular permeability ($0.04 \pm 0{,}02 \times 10^{-4}\%$; n=2) (Figure 36). The administration of 0.01056mg HDL showed a significant increase ($0.6 \pm 0.4 \times 10^{-4}\%$; n=3; p<0.05) indicating a dose dependant permeability increase.

Also in this case increase of vascular permeability starts immediately after application of HDL. Opposite to the other substances permeability continuous to increase without reaching a plateau in the time span measured.

HDL i.v.

▢ HDL 0.01952mg ▪ HDL 0.1056mg
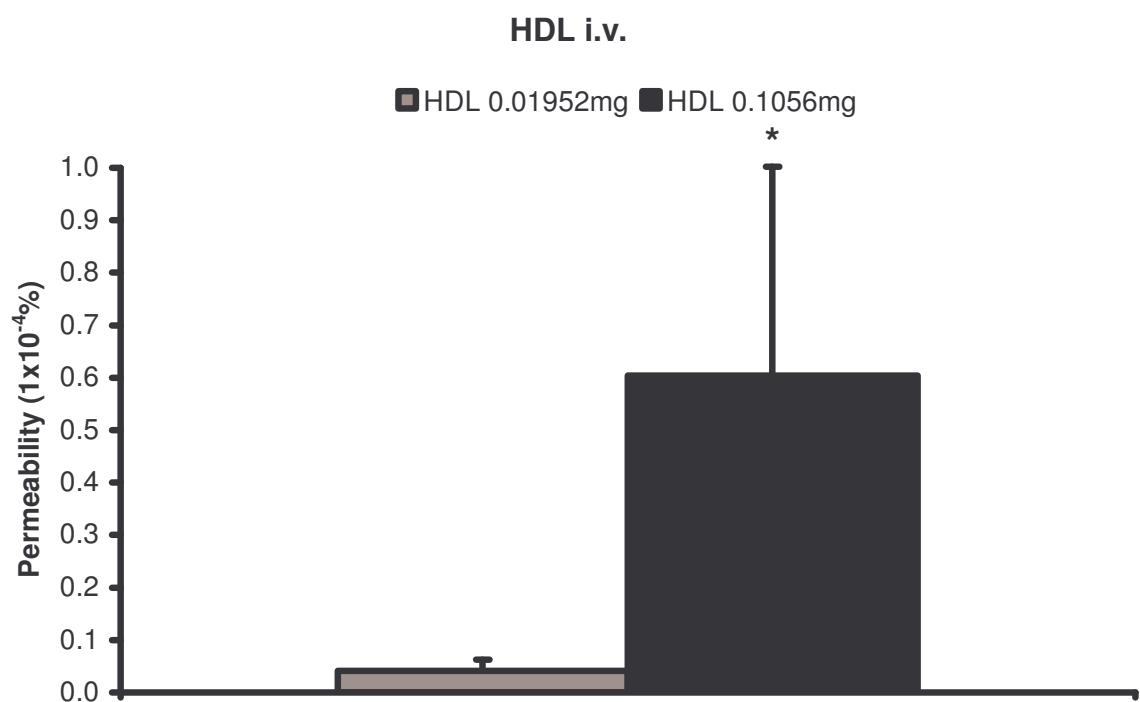
Figure 36. Permeability after administration of 0.01952 mg (n=2) and of 0.1056 mg (n =3) of HDL, respectively

5. Discussion

5.1 Discussion

We report here the morphological and functional dynamics in the multifaceted, time course dependent process of microvascular dysfunction in diabetic mouse model. The results showed that parameters such as vessel density, vessel diameter and permeability are already altered at this early stage, and that glucose, insulin, TRL and HDL have an immediate effect on microcirculation.

This study showed that microvascular alterations do not occur initially when blood glucose levels are pathological, but that microvascular dysfunction is already to be found in early stages of metabolic dysregulation. Since it is known that microvascular dysfunction suffers a sequential development involving the functional and morphological microvascular parameters analysed [17], the changes observed at this early state fit well into the picture of research done in the area of small vessel diseases in diabetic patients.

Some of the observed metabolical alterations found in this study were seen in past studies of 12-week-old UCP1/DTA mice supporting this data. Mean body temperature in UCP1/DTA mice is known to be inferior to that of their control littermates [121]. Body temperature of control animals recovers better from chamber implantation, leading to continuous temperature loss through the ability of metal to conduct heat, mainly to the

fact that UCP1/DTA mice suffer from a deficiency to produce body heat due to the absence of BAT. The temperature drop in both groups and the temperature difference between transgenic and control mice witnessed had been seen in the former study with 20 week old UCP1/DTA mice [1].

The course of bodyweight from UCP1/DTA mice and controls after dorsal window implantation corroborated with previous data [111]. The reduction of bodyweight in UCP1/DTA mice might be related to metabolic alteration linked to the temperature drop of UCP1/DTA mice. It has been shown that weight gain in UCP1/DTA mice strongly depends on the temperature in which they are raised [112]. The initial drop of weight after chamber implantation in both groups, probably related to the surgical intervention, has been documented in previous studies [1, 25]. While control mice stabilise their weight loss after 3 days, UCP1/DTA mice seem to continuously approximate their weight towards the bodyweight of their littermates. This tendency of decreased differences towards the end of the study is notable in almost all of the parameters measured, even though there were no linear correlations found between microvascular parameters and bodyweight.

This could be explained by the fact that in this early stage of metabolical disorder minor weight loss approximates both groups quickly. It has been shown in numerous previous studies, as well as in clinical trials that weight loss can reduce the metabolical disorder at this stage [105]. Therefore the weight loss might explain the differences between day 6 and day 9.

As expected blood glucose levels in UCP1/DTA mice at this early stage did not differ from controls and stayed constant during the observed time span. This situation enabled us to observe the effect of metabolic alterations, such as impaired glucose tolerance, hyperinsulinaemia and dyslipidaemia, in absence of hyperglycaemia. The altered glucose tolerance reassured that metabolical dysfunction is already present at this early stage.

Contrary to a prior study, where no significant difference could be shown between controls and UCP1/DTA mice concerning cholesterol levels in 12 week old male mice [113], we found a significant difference corroborated by the FLPC. The significant increase in triglycerides documented in this study however was also seen in the study von Hamann et al [113]. A possible explanation for the different values found might lay in the different methods used to gain plasma and determine lipoproteins.

The fact that the FLPC showed a pathological distribution of cholesterol and triglycerides in the fractions fit well into the research done in the area of lipoprotein analyse in patients with metabolical syndrome and Type II diabetes concerning vascular dysfunction [77].

When compared to the profound morphological and functional alterations found in the microvascular parameters in 20-week old hyperglycaemic UCP1/DTA mice, the changes documented in this study were minor in their quantity as well as quality, emphasizing the sequential dynamic [17] development of microvascular dysfunction in diabetes.

Amongst the functional microvascular parameters permeability was the most sensitive sign for initial microvascular dysfunctions. These data corroborate other studies in humans [28] as well as animal studies [18, 27], that an elevated vascular permeability towards albumin is an early sign for microvasscular alterations. Although microvascular permeability enables an early assessment of endothelial dysfunction, it has proven to be an inadequate parameter to quantify the severity of microvascular dysfunction in later sages of diabetes, due to the fact that it is highly sensitive and a correlation between the degree of metabolic dysfunction and altered permeability could not be established in hyperglycemic mice [1]. Furthermore, inflammation induced permeability has to be considered as well. UCP1/DTA mice might be more susceptible to inflammatory processes, for instance provoked by the surgery, and the increase of permeability might represent the higher activation of inflammatory processes.

Similar to the previous study done in 20 week old UCP1/DTA mice our data of 12 week old mice showed the same but less intensive pattern of morphological changes with a reduced functional vascular density and increased vascular diameter. Although in younger mice there is a loss of small vessels, there is no shift to larger vessels as in advanced stages. These data support the dynamic element of microvascular alterations in Diabetes.

Even though mean blood flow velocity (V_{mean}) was not significantly altered and mean vessel diameter was enlarged, at this stage mean blood flow rate showed no significant alteration.

This is most probably due to the minor, not significant differences in individual vessels concerning V_{mean}. V_{mean} had been shown in elder mice to be reduced while BFR showed no significant difference. Considering that vessel density is significantly reduced with an equal BFR, the tissue perfusion is most probably already reduced at this early stage of metabolic dysfunction, leading to a lost of substrat delivery due to increased diffusion length. However, due to the equal V_{mean} and increased vessel diameter it is probably less pronounced as in 20 week old mice.

The differences in LEI, evident through the increase in leucocyte cell adhesion in UCP1/DTA mice, were not as strong as in elder mice, where an increased rolling count was additionally observed to an increase in cell adhesion, and vanished in the end of the study. This could be explained by the fact hat in elder mice LEI alterations were found to correlate with high blood glucose levels, which are not present in younger normoglycaemic mice. The initial presence of altered LEI supports the theory that there is an inflammatory component in diabetes and microvascular dysfunction [122, 123]. Leukocyte entrapment is known to occur in diabetes [33-35]. Increased LEI epitomizes inflammatory processes, it may also disturb the balance of leukocyte presence in tissue and therefore may provoke serious complications as seen in wound repair through impaired local inflammatory response. Increased LEI has been

shown to be responsible for ischemia-reperfusion damage in diabetes [18] as well as endothelium dysfunction via inactivation of endothelium-derived relaxing factor such as nitric oxide (NO) through oxygen-derived free radicals [124]. Shear rate playing an important role in LEI [14] as a haemodynamic force, is furthermore not significantly reduced contrary to elder mice. This offers a further explanation to the absence of pronounced LEI.

Permeability in control mice was altered immediately, not only by glucose in a dose dependant form, supporting former data witch showed that endothelial dysfunction correlated with blood glucose values in elder mice, but also by HDL, triglyceride and locally applied insulin supporting that microvascular dysfunction in metabolical syndrome is a multifactorial process, and that there is no necessity of a chronical exposure to the cluster of vascular risk factors to provoke initial vascular dysfunction. The results support former reports that showed increased vascular permeability due to glucose [50, 72], insulin [125, 126] and triglycerides [127].

The dose dependant permeability increase in the stimulation experiments of HDL and TRL, showed that vascular dysfunction can be induced by lower plasma levels then those present in 12 week old mice, not requiring continuously high plasma levels. It has been shown in prior research [79] that postprandial dslipidaemia is present at an early stage of metabolical dysfunction, making the importance of earl treatment to diminish arthreroclerosis evident.

Glucose was not applied locally since the application of a substance with such a high osmolar pressure in a high concentration, necessary due to chamber size not being large enough for a high dilution, would make it difficult to differentiate up to which point the effect on permeability would be due to osmolar effects in the tissue or would is caused by glucose directly. Furthermore since there is an increase in permeability when NaCl is applied, following the manipulation of the glass cover-slip, there might be a mechanical induced permeability increase in this method.

This study emphasis the important of early monitoring of microvascular alterations in diabetic patients, demonstrating that even at an early point, were most patients are not even aware of their metabolic dysfunction, microvascular damage is already occurring. It should be discussed if oral glucose tolerance tests should be performed on obese patients prone to metabolic syndrome so that an early intervention can prevent microvascular complications. Furthermore the effects of the diverse risk factors should be looked into in future studies to determine which therapy against which risk factor has an adequate preventive or even curative effect, at witch stage of microvascular alterations. A conclusion shared by other groups as well [128].

The study furthermore supports the previous research done that demonstrates the positive effect of weight loss and the negative effect of postprandial glucose spikes. The United Kingdom Prospective Diabetes Study (UKPDS) showed that intensive blood glucose control reduced microvascular complications [129].

But as the stimulation experiments of this suggests, an effective management of patients with diabetes requires a treatment directed at correcting all of the abnormalities that increase vascular risk. An opinion sheared by Packard et al in a recent publication [130]. Not only glucose and insulin but also triglycerides should be maintained low to prevent the known effects it has on LDL subclass distribution and size [84]

A possible explanation for escalated atherosclerosis in impaired glucose tolerance and Type 2 diabetes might be the cluster of the metabolic syndrome, which include increased triglycerides, hyperglycaemia, increased high-density lipoprotein cholesterol, high blood pressure and abdominal obesity, preceding and coexisting with diabetes.

The recent publication of a trial approach to prevent cardiovascular disease in people with Type 2 diabetes, suggests that the greatest benefits are seen when glucose, blood pressure and lipid levels are targeted simultaneously [45].

The experiments give us more insights into the mechanism of artherosclerosis, however due to the animal intensive gain of lipid for the injections, this part requires further studies to identify the effects of different lipid fractions.

5.2 Methods Critic

The differences found in the morphological parameters between the prior researched UCP1/DTA mice of 20 week old and the 12 week old animals are quite big, which raises the question what a plausible reason it could have. One possible approach would be the age difference. This is quite improbable since there is no reason why elder control mice should have such an abnormal development of the subcutaneous microvasculature. A more probable explanation would be the individual difference of preparation techniques between different operators, leading to a different layer of subcutaneous tissue observed. This being a systemic error equally existent in the UCP1/DTA and in the control group, since both are prepared by the same person, the results obtained and conclusions derived from these are not affected.

Another point that could be improved in this work would be an increase of animal numbers used especially in the experiment concerning application of glucose, insulin, TRL and HDL. Due to the fact that I wanted to use HDL and TRL from mouse and not from humans, it would have meant a huge number of sacrificed mice to obtain more volume which would have been necessary to elevate the number of experience.

6. Summary

Vascular alterations are the most common causes of morbidity and mortality in diabetic patients. Despite the impact of endothelial dysfunction on microcirculatory properties, little is known about the endothelial cell alteration during the development of diabetes. For that reason we monitored continuously *in vivo* functional and morphological alterations of the micorvasculature in normoglycaemic, hyperinsulinemic and hyperlpidaemic transgenic UCP1/DTA-mice with brown fat deficiency, using a dorsal skin-fold chamber preparation and fluorescence microscopy.

Our results demonstrate functional as well as morphological microvascular alterations in 12 week old UCP1/DTA mice characterized by normoglycaemic values with an impaired glucose-tolerance. Similar, but more advanced alterations have been found in elder UCP1/DTA mice with early stage diabetes. In opposite to 20 week old UCP1/DTA mice, at this early stage of metabolic dysfunction there were no alterations found in parameters such as BFR and LEI. Permeability is already at this stage increased, as well as vessel density, vessel diameter and vessel distribution. In summary these results underline the necessity to recognize and control hyperglycaemic peaks and hyperlipidaemia early, even before there is a clinical status of diabetes mellitus. The microvascular alterations found in the experiments with acute hyperglycaemia, hyperinsulinimia and hyperlipidaemia in control mice, support the role of metabolic parameters in endothelial dysfunction.

7. References

1. Algenstaedt, P., et al., *Microvascular alterations in diabetic mice correlate with level of hyperglycemia.* Diabetes, 2003. **52**(2): p. 542-9.

2. Kannel, W.B. and D.L. McGee, *Diabetes and glucose tolerance as risk factors for cardiovascular disease: the Framingham study.* Diabetes Care, 1979. **2**(2): p. 120-6.

3. Bate, K.L. and G. Jerums, *3: Preventing complications of diabetes.* Med J Aust, 2003. **179**(9): p. 498-503.

4. King, G.L., *The role of hyperglycaemia and hyperinsulinaemia in causing vascular dysfunction in diabetes.* Ann Med, 1996. **28**(5): p. 427-32.

5. Eschwege, E. and B. Balkau, *Hyperglycaemia: link to excess mortality.* Int J Clin Pract Suppl, 2001(123): p. 3-6.

6. Spijkerman, A.M., et al., *Impact of diabetes duration and cardiovascular risk factors on mortality in type 2 diabetes: the Hoorn Study.* Eur J Clin Invest, 2002. **32**(12): p. 924-30.

7. Folkman, J., *Angiogenesis in cancer, vascular, rheumatoid and other disease.* Nat Med, 1995. **1**(1): p. 27-31.

8. Dellian, M., et al., *Quantitation and physiological characterization of angiogenic vessels in mice: effect of basic fibroblast growth factor, vascular endothelial growth factor/vascular permeability factor, and host microenvironment.* Am J Pathol, 1996. **149**(1): p. 59-71.

9. Folkman, J. and Y. Shing, *Angiogenesis.* J Biol Chem, 1992. **267**(16): p. 10931-4.

10. Schaper, W., *Collateral Circulation: Heart, Brain, Kidney, Limbs*, in *Kluwer Academic Publishers*. 1993: Boston.

11. Adamis, A.P., et al., *Increased vascular endothelial growth factor levels in the vitreous of eyes with proliferative diabetic retinopathy.* Am J Ophthalmol, 1994. **118**(4): p. 445-50.

12. Swerlick, R.A., et al., *Regulation of vascular cell adhesion molecule 1 on human dermal microvascular endothelial cells.* J Immunol, 1992. **149**(2): p. 698-705.

13. Haraldsen, G., et al., *Cytokine-regulated expression of E-selectin, intercellular adhesion molecule-1 (ICAM-1), and vascular cell adhesion molecule-1 (VCAM-1) in human microvascular endothelial cells.* J Immunol, 1996. **156**(7): p. 2558-65.

14. Fukumura, D., et al., *Tumor necrosis factor alpha-induced leukocyte adhesion in normal and tumor vessels: effect of tumor type, transplantation site, and host strain.* Cancer Res, 1995. **55**(21): p. 4824-9.

15. Fajardo, L.F., et al., *Dual role of tumor necrosis factor-alpha in angiogenesis.* Am J Pathol, 1992. **140**(3): p. 539-44.

16. Dandona, P., et al., *Tumor necrosis factor-alpha in sera of obese patients: fall with weight loss.* J Clin Endocrinol Metab, 1998. **83**(8): p. 2907-10.

17. Carmeliet, P., *Mechanisms of angiogenesis and arteriogenesis.* Nat Med, 2000. **6**(4): p. 389-95.

18. Panes, J., et al., *Diabetes exacerbates inflammatory responses to ischemia-reperfusion.* Circulation, 1996. **93**(1): p. 161-7.

19. Cheung, A.T., et al., *Microvascular abnormalities in the bulbar conjunctiva of patients with type 2 diabetes mellitus.* Endocr Pract, 2001. **7**(5): p. 358-63.

20. Antonetti, D.A., et al., *Molecular mechanisms of vascular permeability in diabetic retinopathy.* Semin Ophthalmol, 1999. **14**(4): p. 240-8.

21. Lutty, G.A., J. Cao, and D.S. McLeod, *Relationship of polymorphonuclear leukocytes to capillary dropout in the human diabetic choroid.* Am J Pathol, 1997. **151**(3): p. 707-14.

22. Miyamoto, K., et al., *In vivo demonstration of increased leukocyte entrapment in retinal microcirculation of diabetic rats.* Invest Ophthalmol Vis Sci, 1998. **39**(11): p. 2190-4.

23. Bhushan, M., et al., *Recent advances in cutaneous angiogenesis.* Br J Dermatol, 2002. **147**(3): p. 418-25.

24. Price, C.J. and N.P. Brindle, *Vasodilator-stimulated phosphoprotein is involved in stress-fiber and membrane ruffle formation in endothelial cells.* Arterioscler Thromb Vasc Biol, 2000. **20**(9): p. 2051-6.

25. Leunig, M., et al., *Angiogenesis, microvascular architecture, microhemodynamics, and interstitial fluid pressure during early growth of human adenocarcinoma LS174T in SCID mice.* Cancer Res, 1992. **52**(23): p. 6553-60.

26. Domarus, D.V., Deuble-Bente K., *Vaskuläre Erkrankungen der Netzhaut.* In:Böcker W, Denk H, Heitz PhU (Hrgb) Pathologie. 1997, München Wien Baltimore: Urban und Schwarzberg. 340.

27. Antonetti, D.A., et al., *Vascular permeability in experimental diabetes is associated with reduced endothelial occludin content: vascular endothelial growth factor decreases occludin in retinal endothelial cells. Penn State Retina Research Group.* Diabetes, 1998. **47**(12): p. 1953-9.

28. Mogensen, C.E., C.K. Christensen, and E. Vittinghus, *The stages in diabetic renal disease. With emphasis on the stage of incipient diabetic nephropathy.* Diabetes, 1983. **32 Suppl 2**: p. 64-78.

29. Bertoni, A.G., et al., *Diabetes-related morbidity and mortality in a national sample of U.S. elders.* Diabetes Care, 2002. **25**(3): p. 471-5.

30. Charra, B., et al., *Diabetes mellitus in Tassin, France: remarkable transformation in incidence and outcome of ESRD in diabetes.* Adv Ren Replace Ther, 2001. **8**(1): p. 42-56.

31. Lawrence, M.B. and T.A. Springer, *Leukocytes roll on a selectin at physiologic flow rates: distinction from and prerequisite for adhesion through integrins.* Cell, 1991. **65**(5): p. 859-73.

32. Von Andrian, U.H., et al., *L-selectin function is required for beta 2-integrin-mediated neutrophil adhesion at physiological shear rates in vivo.* Am J Physiol, 1992. **263**(4 Pt 2): p. H1034-44.

33. Ashcroft, G.S., et al., *Mice lacking Smad3 show accelerated wound healing and an impaired local inflammatory response.* Nat Cell Biol, 1999. **1**(5): p. 260-6.

34. Danon, D., M.A. Kowatch, and G.S. Roth, *Promotion of wound repair in old mice by local injection of macrophages.* Proc Natl Acad Sci U S A, 1989. **86**(6): p. 2018-20.

35. Leibovich, S.J. and R. Ross, *The role of the macrophage in wound repair. A study with hydrocortisone and antimacrophage serum.* Am J Pathol, 1975. **78**(1): p. 71-100.

36. Schroder, S., W. Palinski, and G.W. Schmid-Schonbein, *Activated monocytes and granulocytes, capillary nonperfusion, and neovascularization in diabetic retinopathy.* Am J Pathol, 1991. **139**(1): p. 81-100.

37. Miyamoto, K., et al., *Prevention of leukostasis and vascular leakage in streptozotocin-induced diabetic retinopathy via intercellular adhesion molecule-1 inhibition.* Proc Natl Acad Sci U S A, 1999. **96**(19): p. 10836-41.

38. Denekamp, J., A. Dasu, and A. Waites, *Vasculature and microenvironmental gradients: the missing links in novel approaches to cancer therapy?* Adv Enzyme Regul, 1998. **38**: p. 281-99.

39. Augustin, H.G., *Tubes, branches, and pillars: the many ways of forming a new vasculature.* Circ Res, 2001. **89**(8): p. 645-7.

40. Patan, S., et al., *Vascular morphogenesis and remodeling in a model of tissue repair: blood vessel formation and growth in the ovarian pedicle after ovariectomy.* Circ Res, 2001. **89**(8): p. 723-31.

41. Patan, S., et al., *Vascular morphogenesis and remodeling in a human tumor xenograft: blood vessel formation and growth after ovariectomy and tumor implantation.* Circ Res, 2001. **89**(8): p. 732-9.

42. Hansen-Algenstaedt, N., et al., *Tumor oxygenation in hormone-dependent tumors during vascular endothelial growth factor receptor-2 blockade, hormone ablation, and chemotherapy.* Cancer Res, 2000. **60**(16): p. 4556-60.

43. Ichioka, S., et al., *Effects of shear stress on wound-healing angiogenesis in the rabbit ear chamber.* J Surg Res, 1997. **72**(1): p. 29-35.

44. Hudlicka, O., *Is physiological angiogenesis in skeletal muscle regulated by changes in microcirculation?* Microcirculation, 1998. **5**(1): p. 5-23.

45. Gaede, P., et al., *Multifactorial intervention and cardiovascular disease in patients with type 2 diabetes.* N Engl J Med, 2003. **348**(5): p. 383-93.

46. Baron, A.D. and G. Brechtel, *Insulin differentially regulates systemic and skeletal muscle vascular resistance.* Am J Physiol, 1993. **265**(1 Pt 1): p. E61-7.

47. *The effect of intensive treatment of diabetes on the development and progression of long-term complications in insulin-dependent diabetes mellitus. The Diabetes Control and Complications Trial Research Group.* N Engl J Med, 1993. **329**(14): p. 977-86.

48. *Epidemiology of Diabetes Interventions and Complications (EDIC). Design, implementation, and preliminary results of a long-term follow-up of the Diabetes Control and Complications Trial cohort.* Diabetes Care, 1999. **22**(1): p. 99-111.

49. *Retinopathy and nephropathy in patients with type 1 diabetes four years after a trial of intensive therapy. The Diabetes Control and Complications Trial/Epidemiology of Diabetes Interventions and Complications Research Group.* N Engl J Med, 2000. **342**(6): p. 381-9.

50.   Hempel, A., et al., *High glucose concentrations increase endothelial cell permeability via activation of protein kinase C alpha.* Circ Res, 1997. **81**(3): p. 363-71.

51.   Schmidt, A.M., et al., *Activation of receptor for advanced glycation end products: a mechanism for chronic vascular dysfunction in diabetic vasculopathy and atherosclerosis.* Circ Res, 1999. **84**(5): p. 489-97.

52.   Mandarino, L.J., *Current hypotheses for the biochemical basis of diabetic retinopathy.* Diabetes Care, 1992. **15**(12): p. 1892-901.

53.   Inoguchi, T., et al., *Preferential elevation of protein kinase C isoform beta II and diacylglycerol levels in the aorta and heart of diabetic rats: differential reversibility to glycemic control by islet cell transplantation.* Proc Natl Acad Sci U S A, 1992. **89**(22): p. 11059-63.

54.   Xia, P., R.M. Kramer, and G.L. King, *Identification of the mechanism for the inhibition of Na+,K(+)-adenosine triphosphatase by hyperglycemia involving activation of protein kinase C and cytosolic phospholipase A2.* J Clin Invest, 1995. **96**(2): p. 733-40.

55.   Chen, S., et al., *High glucose-induced, endothelin-dependent fibronectin synthesis is mediated via NF-kappa B and AP-1.* Am J Physiol Cell Physiol, 2003. **284**(2): p. C263-72.

56.   Hachiya, H., et al., *Regulation of insulin receptor internalization in vascular endothelial cells by insulin and phorbol ester.* J Biol Chem, 1987. **262**(13): p. 6417-24.

57.   Kwok, C., et al., *Identification of persistent defects in insulin receptor structure and function capillary endothelial cells from diabetic rats.* J Clin Invest, 1989. **83**(1): p. 127-36.

58.   Dunlop, M., R. Keogh, and R.G. Larkins, *Fibronectin-induced increase in mesangial cell prostaglandin release. Effect of hyperglycemia and PKC inhibition.* Diabetes, 1993. **42**(1): p. 183-90.

59.   Farese, R.V., et al., *Antisense DNA downregulates protein kinase C isozymes (beta and alpha) and insulin-stimulated 2-deoxyglucose uptake in rat adipocytes.* Antisense Res Dev, 1991. **1**(1): p. 35-42.

60.   Guzman, N.J. and F.T. Crews, *Regulation of inositol transport by glucose and protein kinase C in mesangial cells.* Kidney Int, 1992. **42**(1): p. 33-40.

61.   Mene, P., et al., *High glucose inhibits cytosolic calcium signaling in cultured rat mesangial cells.* Kidney Int, 1993. **43**(3): p. 585-91.

62.   Muller, H.K., et al., *Prevention by protein kinase C inhibitors of glucose-induced insulin-receptor tyrosine kinase resistance in rat fat cells.* Diabetes, 1991. **40**(11): p. 1440-8.

63.   Studer, R.K., P.A. Craven, and F.R. DeRubertis, *Role for protein kinase C in the mediation of increased fibronectin accumulation by mesangial cells grown in high-glucose medium.* Diabetes, 1993. **42**(1): p. 118-26.

64.   Williams, B., *Glucose-induced vascular smooth muscle dysfunction: the role of protein kinase C.* J Hypertens, 1995. **13**(5): p. 477-86.

65.   Derubertis, F.R. and P.A. Craven, *Activation of protein kinase C in glomerular cells in diabetes. Mechanisms and potential links to the pathogenesis of diabetic glomerulopathy.* Diabetes, 1994. **43**(1): p. 1-8.

66.   Koya, D. and G.L. King, *Protein kinase C activation and the development of diabetic complications.* Diabetes, 1998. **47**(6): p. 859-66.

67. Kunisaki, M., et al., *Normalization of diacylglycerol-protein kinase C activation by vitamin E in aorta of diabetic rats and cultured rat smooth muscle cells exposed to elevated glucose levels.* Diabetes, 1994. **43**(11): p. 1372-7.

68. Koya, D., et al., *Characterization of protein kinase C beta isoform activation on the gene expression of transforming growth factor-beta, extracellular matrix components, and prostanoids in the glomeruli of diabetic rats.* J Clin Invest, 1997. **100**(1): p. 115-26.

69. Craven, P., R. Studer, and F. DeRubertis, *Impaired nitric oxide-dependent cyclic guanosine monophosphate generation in glomeruli from diabetic rats. Evidence for protein kinase C-mediated suppression of the cholinergic response.* J Clin Invest, 1994. **93**(1): p. 311-20.

70. Chiarelli, F., F. Santilli, and A. Mohn, *Role of growth factors in the development of diabetic complications.* Horm Res, 2000. **53**(2): p. 53-67.

71. Kawagishi, T., et al., *Impaired endothelium-dependent vascular responses of retinal and intrarenal arteries in patients with type 2 diabetes.* Arterioscler Thromb Vasc Biol, 1999. **19**(10): p. 2509-16.

72. Haller, H., *Postprandial glucose and vascular disease.* Diabet Med, 1997. **14 Suppl 3**: p. S50-6.

73. Yudkin, J.S., *Hyperinsulinaemia, insulin resistance, microalbuminuria and the risk of coronary heart disease.* Ann Med, 1996. **28**(5): p. 433-8.

74. Baron, A.D., *Hemodynamic actions of insulin.* Am J Physiol, 1994. **267**(2 Pt 1): p. E187-202.

75. Grant, M.K., GL., *IGF-1 and blood vessels. Implications for microvascular and macrovascular disease.* Diabetes Rev, 1995. **3**: p. 113-28.

76. Ginsberg, H.N., *Lipoprotein physiology in nondiabetic and diabetic states. Relationship to atherogenesis.* Diabetes Care, 1991. **14**(9): p. 839-55.

77. Temelkova-Kurktschiev, T. and M. Hanefeld, *The lipid triad in type 2 diabetes - prevalence and relevance of hypertriglyceridaemia/low high-density lipoprotein syndrome in type 2 diabetes.* Exp Clin Endocrinol Diabetes, 2004. **112**(2): p. 75-9.

78. Siegel, R., et al., *Lipoproteins, apolipoproteins, and low-density lipoprotein size among diabetics in the Framingham offspring study.* Metabolism, 1996. **45**(10): p. 1267-72.

79. Henkel, E., et al., *[Predictors of abnormal glucose tolerance in persons at risk of type 2 diabetes: the RIAD study].* Dtsch Med Wochenschr, 2002. **127**(18): p. 953-7.

80. Iso, H., et al., *Serum triglycerides and risk of coronary heart disease among Japanese men and women.* Am J Epidemiol, 2001. **153**(5): p. 490-9.

81. Jeppesen, J., et al., *Triglyceride concentration and ischemic heart disease: an eight-year follow-up in the Copenhagen Male Study.* Circulation, 1998. **97**(11): p. 1029-36.

82. Krentz, A.J., *Lipoprotein abnormalities and their consequences for patients with type 2 diabetes.* Diabetes Obes Metab, 2003. **5 Suppl 1**: p. S19-27.

83. Sacks, F.M., et al., *The effect of pravastatin on coronary events after myocardial infarction in patients with average cholesterol levels.*

Cholesterol and Recurrent Events Trial investigators. N Engl J Med, 1996. **335**(14): p. 1001-9.

84. Fabryova, L. and S. Cagan, *[Relation between insulin resistance and small, dense lipoproteins with low density and the development of atherosclerosis in type 2 diabetes mellitus].* Bratisl Lek Listy, 1998. **99**(3-4): p. 138-45.

85. Pedersen, T.R. and J.A. Tobert, *Simvastatin: a review.* Expert Opin Pharmacother, 2004. **5**(12): p. 2583-96.

86. Li, H., et al., *An atherogenic diet rapidly induces VCAM-1, a cytokine-regulatable mononuclear leukocyte adhesion molecule, in rabbit aortic endothelium.* Arterioscler Thromb, 1993. **13**(2): p. 197-204.

87. Hessler, J.R., et al., *Lipoprotein oxidation and lipoprotein-induced cytotoxicity.* Arteriosclerosis, 1983. **3**(3): p. 215-22.

88. Steinberg, D., *Atherogenesis in perspective: hypercholesterolemia and inflammation as partners in crime.* Nat Med, 2002. **8**(11): p. 1211-7.

89. Libby, P., *Inflammation in atherosclerosis.* Nature, 2002. **420**(6917): p. 868-74.

90. Navab, M., et al., *High density associated enzymes: their role in vascular biology.* Curr Opin Lipidol, 1998. **9**(5): p. 449-56.

91. Yuan, F., et al., *Microvascular permeability of albumin, vascular surface area, and vascular volume measured in human adenocarcinoma LS174T using dorsal chamber in SCID mice.* Microvasc Res, 1993. **45**(3): p. 269-89.

92. Fukumura, D., et al., *Effect of host microenvironment on the microcirculation of human colon adenocarcinoma.* Am J Pathol, 1997. **151**(3): p. 679-88.

93. Sasaki, A., et al., *Preferential localization of human adherent lymphokine-activated killer cells in tumor microcirculation.* J Natl Cancer Inst, 1991. **83**(6): p. 433-7.

94. Ohkubo, C., D. Bigos, and R.K. Jain, *Interleukin 2 induced leukocyte adhesion to the normal and tumor microvascular endothelium in vivo and its inhibition by dextran sulfate: implications for vascular leak syndrome.* Cancer Res, 1991. **51**(5): p. 1561-3.

95. Nugent, L.J. and R.K. Jain, *Extravascular diffusion in normal and neoplastic tissues.* Cancer Res, 1984. **44**(1): p. 238-44.

96. Zawicki, D.F., et al., *Dynamics of neovascularization in normal tissue.* Microvasc Res, 1981. **21**(1): p. 27-47.

97. Dudar, T.E. and R.K. Jain, *Microcirculatory flow changes during tissue growth.* Microvasc Res, 1983. **25**(1): p. 1-21.

98. Melder, R.J., et al., *Selectin- and integrin-mediated T-lymphocyte rolling and arrest on TNF-alpha-activated endothelium: augmentation by erythrocytes.* Biophys J, 1995. **69**(5): p. 2131-8.

99. Melder, R.J., H.A. Salehi, and R.K. Jain, *Interaction of activated natural killer cells with normal and tumor vessels in cranial windows in mice.* Microvasc Res, 1995. **50**(1): p. 35-44.

100. Hansen-Algenstaedt, N., et al., *Long-term observation reveals time-course-dependent characteristics of tumour vascularisation.* Eur J Cancer, 2005. **41**(7): p. 1073-85.

101. Hansen-Algenstaedt, N., et al., *Femur window-a new approach to microcirculation of living bone in situ.* J Orthop Res, 2005.

102. Lowell, B.B., et al., *Development of obesity in transgenic mice after genetic ablation of brown adipose tissue.* Nature, 1993. **366**(6457): p. 740-2.

103. Hamann, A., et al., *Characterization of insulin resistance and NIDDM in transgenic mice with reduced brown fat.* Diabetes, 1995. **44**(11): p. 1266-73.

104. Mardarowicz, G., J. Lopatynski, and T. Nicer, *Metabolic syndrome.* Ann Univ Mariae Curie Sklodowska [Med], 2003. **58**(1): p. 426-31.

105. Case, C.C., et al., *Impact of weight loss on the metabolic syndrome.* Diabetes Obes Metab, 2002. **4**(6): p. 407-14.

106. Himms-Hagen, J., *Brown adipose tissue thermogenesis and obesity.* Prog Lipid Res, 1989. **28**(2): p. 67-115.

107. Himms-Hagen, J., *Brown adipose tissue thermogenesis: interdisciplinary studies.* Faseb J, 1990. **4**(11): p. 2890-8.

108. Nicholls, D.G. and R.M. Locke, *Thermogenic mechanisms in brown fat.* Physiol Rev, 1984. **64**(1): p. 1-64.

109. Klaus, S., et al., *The uncoupling protein UCP: a membraneous mitochondrial ion carrier exclusively expressed in brown adipose tissue.* Int J Biochem, 1991. **23**(9): p. 791-801.

110. Tritos, N.A., et al., *Characterization of expression of hypothalamic appetite-regulating peptides in obese hyperleptinemic brown adipose tissue-deficient (uncoupling protein-promoter-driven diphtheria toxin A) mice.* Endocrinology, 1998. **139**(11): p. 4634-41.

111. Melnyk, A., M.E. Harper, and J. Himms-Hagen, *Raising at thermoneutrality prevents obesity and hyperphagia in BAT-ablated transgenic mice.* Am J Physiol, 1997. **272**(4 Pt 2): p. R1088-93.

112. Melnyk, A. and J. Himms-Hagen, *Temperature-dependent feeding: lack of role for leptin and defect in brown adipose tissue-ablated obese mice.* Am J Physiol, 1998. **274**(4 Pt 2): p. R1131-5.

113. Hamann, A., J.S. Flier, and B.B. Lowell, *Decreased brown fat markedly enhances susceptibility to diet-induced obesity, diabetes, and hyperlipidemia.* Endocrinology, 1996. **137**(1): p. 21-9.

114. Havel, R.J., H.A. Eder, and J.H. Bragdon, *The distribution and chemical composition of ultracentrifugally separated lipoproteins in human serum.* J Clin Invest, 1955. **34**(9): p. 1345-53.

115. Goldstein, J.L., S.K. Basu, and M.S. Brown, *Receptor-mediated endocytosis of low-density lipoprotein in cultured cells.* Methods Enzymol, 1983. **98**: p. 241-60.

116. Lehr, H.A., et al., *Dorsal skinfold chamber technique for intravital microscopy in nude mice.* Am J Pathol, 1993. **143**(4): p. 1055-62.

117. Yuan, F., et al., *Vascular permeability and microcirculation of gliomas and mammary carcinomas transplanted in rat and mouse cranial windows.* Cancer Res, 1994. **54**(17): p. 4564-8.

118. Lipowsky, H.H. and B.W. Zweifach, *Application of the "two-slit" photometric technique to the measurement of microvascular volumetric flow rates.* Microvasc Res, 1978. **15**(1): p. 93-101.

119. Yuan, F., et al., *Microvascular permeability and interstitial penetration of sterically stabilized (stealth) liposomes in a human tumor xenograft.* Cancer Res, 1994. **54**(13): p. 3352-6.

120. Brizel, D.M., et al., *A comparison of tumor and normal tissue microvascular hematocrits and red cell fluxes in a rat window chamber model.* Int J Radiat Oncol Biol Phys, 1993. **25**(2): p. 269-76.

121. Klaus, S., et al., *Physiology of transgenic mice with brown fat ablation: obesity is due to lowered body temperature.* Am J Physiol, 1998. **274**(2 Pt 2): p. R287-93.

122. Das, U.N., *Is metabolic syndrome X an inflammatory condition?* Exp Biol Med (Maywood), 2002. **227**(11): p. 989-97.

123. Engstrom, G., et al., *Inflammation-sensitive plasma proteins, diabetes, and mortality and incidence of myocardial infarction and stroke: a population-based study.* Diabetes, 2003. **52**(2): p. 442-7.

124. Rubanyi, G.M. and P.M. Vanhoutte, *Superoxide anions and hyperoxia inactivate endothelium-derived relaxing factor.* Am J Physiol, 1986. **250**(5 Pt 2): p. H822-7.

125. Kalambokis, G.N., A.A. Tsatsoulis, and E.V. Tsianos, *The edematogenic properties of insulin.* Am J Kidney Dis, 2004. **44**(4): p. 575-90.

126. Bent-Hansen, L., et al., *Transcapillary escape rate and relative metabolic clearance of glycated and non-glycated albumin in type 1 (insulin-dependent) diabetes mellitus.* Diabetologia, 1987. **30**(1): p. 2-4.

127. Jagla, A. and J. Schrezenmeir, *Postprandial triglycerides and endothelial function.* Exp Clin Endocrinol Diabetes, 2001. **109**(4): p. S533-47.

128. Alebiosu, C.O. and B.O. Odusan, *Metabolic syndrome in subjects with type-2 diabetes mellitus.* J Natl Med Assoc, 2004. **96**(6): p. 817-21.

129. *Intensive blood-glucose control with sulphonylureas or insulin compared with conventional treatment and risk of complications in patients with type 2 diabetes (UKPDS 33). UK Prospective Diabetes Study (UKPDS) Group.* Lancet, 1998. **352**(9131): p. 837-53.

130. Packard, C. and A.G. Olsson, *Management of hypercholesterolaemia in the patient with diabetes.* Int J Clin Pract Suppl, 2002(130): p. 27-32.

11.Anhang

11.1 Abbildungsverzeichnis

11.2 Abkürzungsverzeichnis

aFGF	**a**cidic **F**ibroblast **G**rowth **F**actor
BAT	**b**rown **a**dipose **t**issue
bFGF	**b**asic **F**ibroblast **G**rowth **F**actor
BFR	**B**lood **F**low **R**ate
CAMs	**C**ell **A**dhesion **M**olecules
CCD	**c**harge **c**ouple **d**evice camera
D	Vascular **D**iameter
DAG	**dia**cyl**g**lcerol
DCCT	**D**iabetes **C**ontrol and **C**omplication **T**rial
EDIC	**E**pidemiology of **D**iabetes **I**nterventions and **C**omplications
EGF	**e**pidermal **g**rowth **f**actor
FITC-Dextran	**f**luorescein **i**sothiocyanate **d**extran
FPLC	**f**ast **p**erformance **l**iquid **c**hromatography gel filtration
GF	**g**rowth **f**actors
GGT	**g**lucose-**t**olerance-**t**ests
HDL	**h**igh-**d**ensity **l**ipoprotein
HT	**h**eama**t**ocrit
ICAM-1	**I**ntercellular **A**dhesion **M**olecule **1**
IGF-1	**i**nsulin-like **G**rowth **F**actor **1**
IgG	**i**mmun**g**lobulin **G**
IL-1 beta	**i**nter**l**eukin-1 beta

LDL	**l**ow-**d**ensity **l**ipoprotein
LEI	**L**eukocyte-**E**ndothelial-**I**nteraction
MS	**m**etabolical **s**yndrome
NCEP	**N**ational **c**holesterol **e**ducation **p**rogram
NEFA	**n**onesterified **f**atty **a**cids
OGTT	**o**ral **g**lucose **t**olerance **t**est
OxLDL	**ox**idized **l**ow-**d**ensity **l**ipoprotein
P	**p**ermeability
PKC	**p**rotein **k**inase **C**
RBC	**r**ed **b**lood **c**ell velocity
Rho-6-G	tetramethyl**rho**damine
RIAD	**R**isk Factors in **I**mpaired Glucose Tolerance for **A**therosclerosis and **D**iabetes study
SEM	**s**tandard **e**rror of the **m**ean
SV	**S**urface/**V**olume
TG	**t**ri**g**lycerides
TRL	**t**riglyceride-**r**ich **l**ipoprotein
TNF-α	**t**umor-**n**ecrosis **f**actor alpha
TRITC-BSA	**t**et**r**amethylrhodamine labeled **b**ovine **s**erum **a**lbumin
UCP1/DTA	**U**n**c**oupling **p**rotein promoter-driven **d**iphteria **t**oxin **A**
VCAM-1	**v**ascular **c**ell **a**dhesion **m**olecule 1
VD	Functional **V**ascular **D**ensity
VEGF	**v**ascular **e**ndothelial **g**rowth **f**actor
V_{mean}	**mean** blood flow **v**elocity
V_{RBC}	**R**ed **b**lood **c**ell **v**elocity

8. Danksagung

9. Lebenslauf

Tanja Biermann, geboren am 29.12.1974 in Singapur

Schulausbildung

08/1980-05/1993	Deutsche Schule in Singapur, Vereinigte Arabische Emirate, Deutschland und Portugal

Universitätsausbildung

10/1993-03/1996	Wirtschaftsinformatik, Lissabon, Portugal
04/1996-11/2002	Humanmedizin, Universitätsklinikum Hamburg – Eppendorf
03/1998	Ärztliche Vorprüfung
03/1999	Erster Abschnitt der Ärztlichen Prüfung
08/2001	Zweiter Abschnitt der Ärztlichen Prüfung
11/2002	Ärztliche Prüfung
06/2004	Approbation
10/2001-09/2002	Praktisches Jahr: Frauenklinik/UKE, Innere/AK St. Georg ,Chirurgie/ Marienkrankenhaus

Famulaturen und Praktika

1996	Acht Wochen Krankenpflegepraktikum im Hospital Santa Maria in Lissabon
1998	Medizinische Abteilung im Mercy Hospital in Cork/Irland
1999	Unfallchirugie, Marienkrankenhaus in Hamburg
2000	Notaufnahme, Kalafong Hospital in Pretoria/Südafrika
2001	Clínica Europa, Portugal

Beruflicher Werdegang

01/2003-06/2004	Klinik und Poliklinik für Orthopädie, Universitätsklinikum Hamburg-Eppendorf
09/3004-03/2005	Klinik für Orthopädie, Rheumaklinik Bad Bramstedt

Publikationen:

02/2003	Mikrovascular Alterations in Diabetic Mice Correlate With Level of Hperglycemia; (Diabetes, Vol. 52(2); 542-549, February 2003)
05/2005	Long-term observation reveals time-course-dependent characteristics of tumour vascularisation; (Eurt J Cancer, Vol 41(7); 1073-85, May 2005)

Vortrag:

Nov. 2003	Pathologische Glucosetoleranz ist assoziiert mit incipienten inflammatorischen mikrovaskulären Veränderungen - Deutscher Orthopädenkongress DGOOC in Berlin

Poster award:

Nov. 2002	Microvascular Alterations in diabetic mice: a target for somatostatin analogue therapy Somatostatin Receptors and Targets for Therapy with Somatostatin Analogues - A Young Investigator Meeting in Barcelona

Posterpräsentationen:

Mai 2001	Intravital Monitoring of Insulin Related Microvascular Dysfunktions Rationalizes Anti-Angiogenetic Therapy VIIIth International Symposium on Insulin - Receptors and Insulin Action in Genf
Feb. 2002	Diabetes Specific Morphological and FunctionalMicrovascular Alterations, Keystone Symposia – Angiogenesis in Cancer and other Diseases: From Genes to Funktion to Therapy

Hamburg, 22.06.2005

10. Erklärung

Ich versichere ausdrücklich, dass ich die Arbeit selbstständig und ohne fremde Hilfe verfasst, andere als. die von mir angegebenen Quellen und Hilfsmittel nicht benutzt und die aus den benutzten Werken wörtlich oder inhaltlich entnommenen Stellen einzeln nach Ausgabe (Auflage und Jahr des Erscheinens), Band und Seite des benutzten Werkes kenntlich gemacht habe.

Ferner versichere ich, dass ich die Dissertation bisher nicht an einem Fachvertreter an einer anderen Hochschule zur Überprüfung vorgelegt oder mich anderweitig um Zulassung zur Promotion beworben habe.

....